

# **Estimating Internal Moisture Generation Rates in Recently Constructed, Occupied Homes in the Southeastern US**

Internal moisture generation (IMG), or moisture generated by building occupants via activities such as respiration, cooking, bathing, and cleaning, is a critical input required for design, analysis, and simulation of building enclosure and heating, ventilation, and air conditioning (HVAC) systems. Based on previously published values, ASHRAE Standard 160-2021 provides guidance for estimating IMG rates for moisture control design analysis, which is based on occupied home datasets collected in the 1980s and 1990s. Residential energy use simulation software also utilizes estimates for IMG for energy rating, energy analysis, and code compliance calculations, as specified in ANSI/RESNET/ICC Standard 301. Data quantifying IMG rates in newer homes is useful in determining the continued relevance of current design and simulation guidance, and whether the guidance represents conditions found in new housing stock.

ASHRAE Research Project 1844, conducted by the Florida Solar Energy Center (FSEC), a research institute of the University of Central Florida, estimated IMG rates in newer occupied homes built since 2013 in the southeastern US using a moisture balance model approach. The project obtained occupied home data in cooperation with a US Department of Energy Building America research project to characterize indoor air quality (IAQ) in newer US homes, along with presence, functionality, and occupant use of control measures. Full-scale laboratory homes operating with known IMG rates were used to validate a moisture balance model and quantify the accuracy of estimates obtained when the model is applied to data from occupied homes with unknown IMG rates.

Keywords: internal moisture, moisture balance, moisture buffering, diffusion, ventilation

## **Introduction**

Internal moisture generation (IMG), or moisture generated by building occupants via activities such as respiration, cooking, bathing, and cleaning, is a critical input required for design, analysis, and simulation of building enclosure and heating, ventilation, and air conditioning (HVAC) systems. Other factors influencing the overall moisture load in

a home include natural and mechanical ventilation, mechanical humidification/dehumidification, diffusion through building assemblies, and sorption in and out of building materials and furnishings. Based on previously published values, ASHRAE Standard 160-2021 (ASHRAE 2021) provides guidance for estimating IMG for moisture control design analysis, which is based on occupied home datasets collected in the 1980s and 1990s. Residential energy use simulation software also utilizes estimates for IMG for energy rating, energy analysis, and code compliance calculations, as specified in ANSI/RESNET/ICC Standard 301 (ANSI 2019). Data quantifying IMG rates in newer homes is useful in determining the continued relevance of current design and simulation guidance, and whether the guidance represents conditions found in new housing stock.

ASHRAE Research Project 1844, conducted by the Florida Solar Energy Center (FSEC), a research institute of the University of Central Florida, estimated IMG rates in newer occupied homes built since 2013 in the southeastern US. Full-scale laboratory homes operating with known IMG rates were used to validate a moisture balance model and quantify the accuracy of estimates obtained when the model is applied to data from occupied homes with unknown IMG rates. Some of this validation work is described in Martin et al. (2022), and this journal paper represents an extended version of that previously published conference paper.

ASHRAE Research Project 1844 obtained occupied home data in cooperation with a US Department of Energy Building America research project to characterize indoor air quality (IAQ) in newer US homes, along with presence, functionality, and occupant use of control measures. The Building America IAQ (BAIAQ) study engaged research teams to collect data regionally: Pacific Northwest National Laboratory in OR and CO, representing marine and cold dry climates, University of Illinois Urbana-

Champaign in IL representing cold climate, and FSEC in FL, GA, and SC representing warm humid climates. Martin et al. (2020) describes preliminary data from the project focusing on characterization of whole house mechanical ventilation (WHMV) systems found in some of the homes. Published results for the full study are forthcoming, along with a publicly accessible database. All teams used the same base data collection protocol, but the FSEC team added some additional measurements specifically for the purpose of estimating IMG rates, including measurement of air conditioning/dehumidification condensate, and tracer gas testing to better quantify infiltration rates and duct leakage. Therefore, only data from homes in the southeastern US in which the expanded protocol could be carried out have been used to estimate IMG rates. The BIAAQ project had planned to estimate IMG rates in a limited number of homes, and ASHRAE funding expanded analysis to a greater number of homes.

## **Background**

To quantify IMG in occupied homes, different measurement approaches can be used. One approach is to measure the rate of moisture generated by individual occupant activities. Due to inherent difficulty with this direct form of measurement, another indirect approach that can be used involving measurement of other dominant, non-occupant related moisture addition and removal mechanisms, and then applying a moisture balance model to calculate an estimated total, occupant-related, IMG rate. The US Forest Products Laboratory (FPL) prepared a summary of moisture balance models used to predict indoor relative humidity, including a literature review of available data on IMG rates (Glass and TenWolde 2009). One finding is that available data relating IMG rates to numbers of occupants varies significantly (Figure 1).

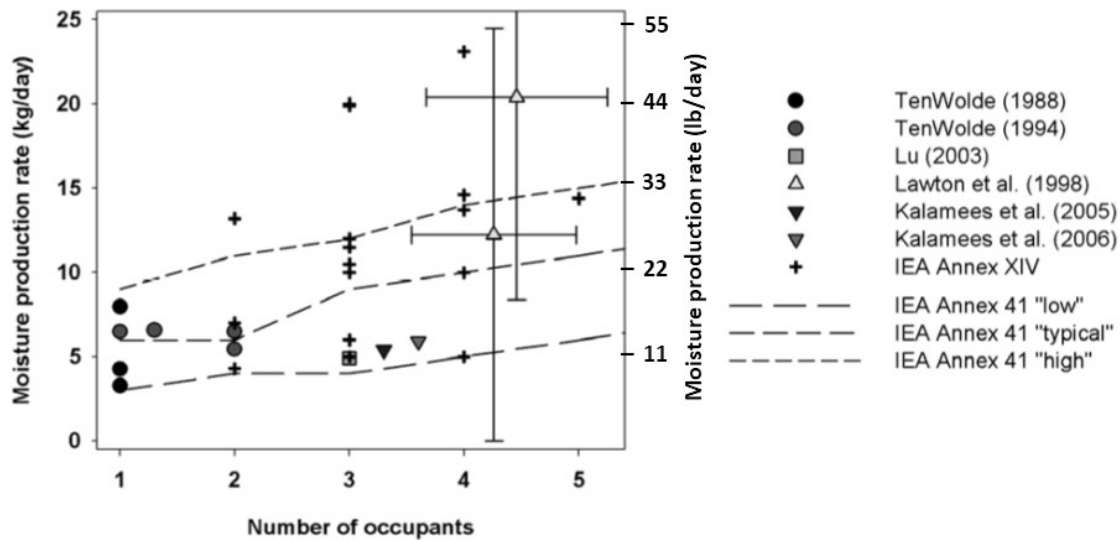


Figure 1. IMG rates from literature (Glass and TenWolde 2009). IEA values (dashed lines and + symbols) represent measurement and summation of individual internal moisture sources. Other symbols represent whole house estimates calculated with moisture balance models.

One reason the IMG rates vary is the inherent variability in occupant lifestyles (Pallin 2017) and interactions with building technologies. Another reason is that relative contribution of individual moisture sources to the total internally generated moisture load may vary over time. For example, the FPL report states it was previously assumed that clothes washing is a significant source of internal moisture, but it could now be assumed that clothes washing and cleaning can likely be ignored as contributors to internal moisture load in modern homes. The authors of the FPL report call for the need for additional measurements to determine whether current estimates used for IMG rates in design procedures should be adjusted.

### Baseline Moisture Balance Model

A baseline moisture balance model was developed for a zone without consideration of diffusion or moisture absorbing surfaces:

$$m_z \frac{d\omega_z}{dt} = \dot{m}_{da,v}(\omega_o - \omega_z) + \dot{m}_g - \dot{m}_c \quad (1)$$

This equation expresses the rate of change in mass of moisture in the zone ( $m_z \frac{d\omega_z}{dt}$ ) as a function of moisture added or removed due to air exchange with outdoors ( $\dot{m}_{da,v}(\omega_o - \omega_z)$ ), moisture added due to IMG ( $\dot{m}_g$ ), and moisture removed via air conditioning or dehumidification condensate production ( $\dot{m}_c$ ). An analytical solution provides an equation for IMG as a function of the other major moisture flows.

$$\dot{m}_g = \dot{m}_c - \dot{m}_{da,v}\omega_o + (\dot{m}_{da,v}) \left[ \frac{\omega_z^t - \omega_z^{t-1} e^{-\frac{\dot{m}_{da,v}t}{m_z}}}{1 - e^{-\frac{\dot{m}_{da,v}t}{m_z}}} \right] \quad (2)$$

Unlike IMG, these other moisture flows can be measured with relative ease and accuracy in lab home and occupied home settings. Measurement techniques utilized for the lab homes follows, with similar techniques employed in the occupied homes discussed later in this paper. Methods utilized to estimate other moisture flows that are difficult to measure directly including material sorption and diffusion through building materials are also discussed.

### **Lab Home Experimentation to Validate the Moisture Balance Model**

For model validation, data was collected in two simulated occupancy lab homes located on the FSEC campus in Cocoa, FL. The first is the Flexible Residential Test Facility (FRTF), a 143 m<sup>2</sup> (1,536 ft<sup>2</sup>) single-story, site built residential structure shown in Figure 2. The slab-on-grade building was built in 2010 and designed to mimic a typical Florida existing home. It has painted, uninsulated concrete block walls with no exterior cladding, single pane windows, and a vented attic with shingle roof covering and R-19 kraft-faced fiberglass batt ceiling insulation. The space conditioning system is a SEER 16, two-stage heat pump with air handler located in the garage and flexible ductwork

located in the attic. While designed as a three bedroom, two bathroom home, the interior floor plan was never built out resulting in a single, well-mixed indoor space. Interior wall modules were constructed with the same type and amount of material as interior walls, and placed inside the space for heat and moisture capacitance. Half of the slab floor is left exposed to the space, and half is covered with carpet and pad.



Figure 2. Flexible Residential Test Facility (FRTF).

The second is the Manufactured Housing Laboratory (MH Lab), a 149 m<sup>2</sup> (1,600 ft<sup>2</sup>) single-story factory-built home shown in Figure 3. The three-bedroom, two-bathroom home was manufactured in 2001 and was constructed according to the US Environmental Protection Agency Energy Star Program for manufactured homes. The MH Lab has R-13 wood frame walls with vinyl siding, single pane windows, a vented attic with R-30 blown cellulose insulation, a sealed crawlspace with R-19 fiberglass batt floor insulation, and a SEER 13 heat with pump with indoor located air handler and duct work. Unlike the FRTF, this home is fully furnished with tables, chairs, couches, and beds, and has carpet in all rooms except the kitchen and bathrooms which have tile floor covering.



Figure 3. Manufactured Housing Lab (MH Lab).

The internal sensible and latent heat gain schedules were set to approximate the Building America Benchmark hourly schedules (Fang 2011). In the FRTF, heat lamps generated sensible internal load, and a calibrated ultrasonic humidifier was utilized to generate internal latent load. In the MH Lab, sensible internal load was generated by a combination of oven operation and heat lamps, and latent internal load was generated in the kitchen area and in the master bathroom by a calibrated system that evaporated water with heat sources. During the course of data collection, the latent gain schedule was periodically adjusted to intentionally simulate varying IMG rates expected in occupied homes. Neither lab has any fan forced air circulation other than that resulting from the operation of the central forced air space conditioning system.

A summary of lab instrumentation and measurements is shown in Table 1. Air conditioning condensate from each lab is monitored using tipping buckets that have

been calibrated in-situ. Measurements of indoor temperature (T) and relative humidity (RH) are used to calculate the humidity ratio ( $\omega$ ).

Table 1. Summary of lab home measurements and instrumentation.

Measurement	Equipment	Measurement Interval	Accuracy
Data acquisition	Campbell Scientific CR3000 and CR1000 data logger	30 sec sampling	0.06% of analog input reading
Indoor and outdoor temperature and relative humidity	Vaisala HMP60 (Thin-film, dielectric capacitive)	15 min	$\pm 0.5^{\circ}\text{C}$ , $\pm 3\%$ RH
Wind speed	Three cup anemometer	15 min	1.5% of reading (mph)
Condensate	Texas Instruments Tipping Bucket	15 min	1% of reading (in/hour)
Building envelope and duct system air leakage	Minneapolis Blower Door System with DG-700 digital gauge	Single measurement	3% of result (cfm at 50 pascals)
	Miran sulfur hexafluoride (SF <sub>6</sub> ) specific gas analyzer	Single measurement	$\pm 10\%$ (SF <sub>6</sub> Detection Limit = 10 ppb)

In the FRTF, indoor T and RH were monitored in one central location by a sensor hanging in the middle of the air mass with the thermostat. Figure 4 shows the location of the internal moisture source, and indoor T/RH measurement for the FRTF, overlaid on the designed (but not built-out) interior floor plan.

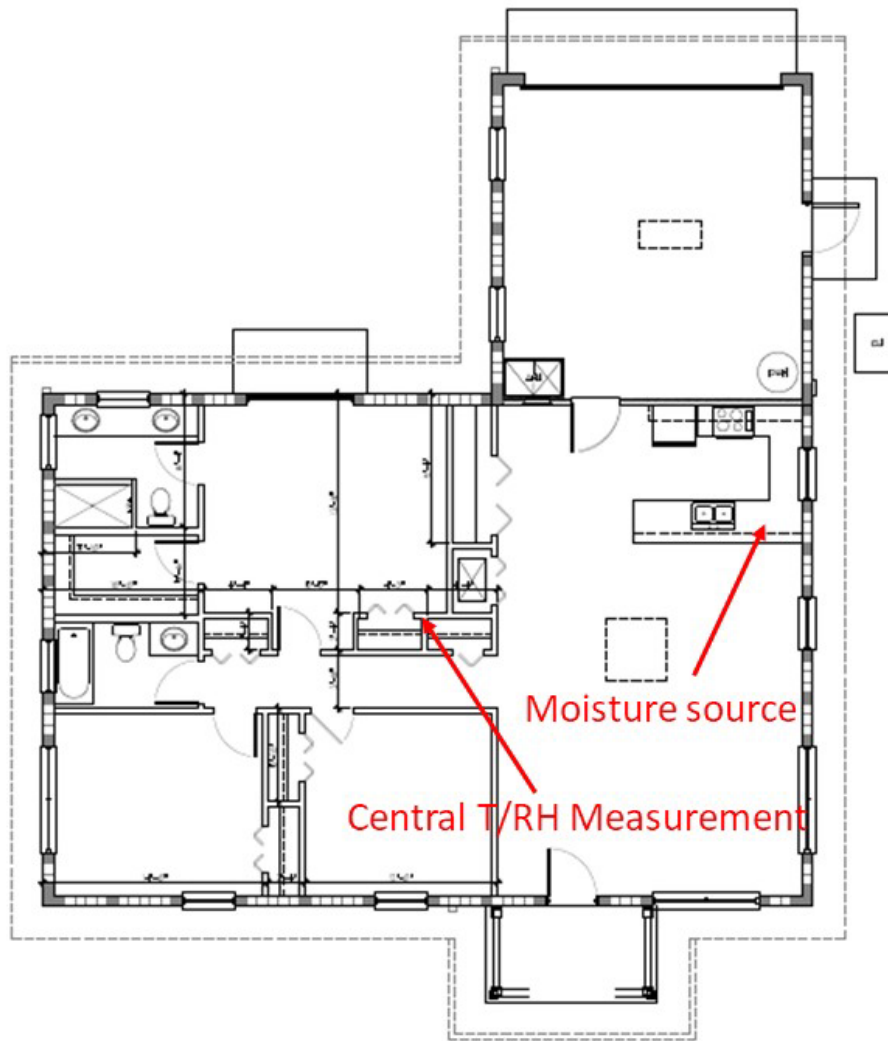


Figure 4. FRTF floor plan showing location of internal moisture source and indoor T/RH measurement (interior walls not present in lab).

In the MH lab, indoor T and RH are measured with similar sensors in multiple locations: in the living room near the thermostat, in the utility room, and in each of the three bedrooms. The volume of each space is calculated, and a single humidity ratio representing the whole house is determined using a volume-weighted average. The volume assigned to the central living area measurement includes all spaces not directly monitored. Figure 5 shows the locations of the MH Lab internal moisture sources and indoor T/RH measurements overlaid on the interior floor plan.

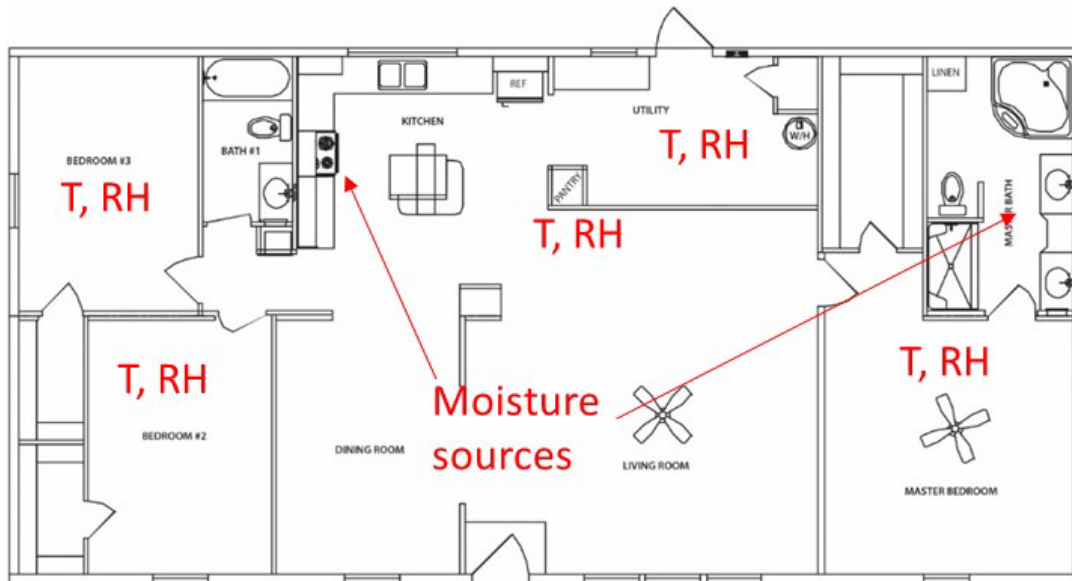


Figure 5. MH Lab floor plan showing location of internal moisture sources and indoor T/RH measurements.

Outdoor T and RH are measured at a weather station in close proximity to the labs and utilized along with a calculated total air exchange rate to determine the contribution of moisture from air exchange with outdoors. To determine the natural infiltration portion of this rate, a blower door test was conducted to determine the flow coefficient and flow exponent for each lab. The FRTF was designed with provisions to adjust envelope leakage, and for these experiments was configured to represent a tighter building with an air changes per hour at 50 pascals (ACH50) of 2.5. The MH Lab is a leakier building, with ACH50 of 5.0. As discussed later in this paper, envelope leakage of occupied homes falls within this range. The flow coefficient and exponent obtained from the blower door results are used along with monitored indoor/outdoor temperatures and wind speed to calculate the wind and stack driven components of natural infiltration using the ASHRAE enhanced model procedure found in Appendix C of ASHRAE Standard 62.2-2022 (ASHRAE 2022). A tracer gas decay test was conducted in each lab and a non-linear solving method was used to calibrate the natural

infiltration model coefficients so that the calculated natural infiltration rate aligned with the one-time measurement of infiltration conducted with a tracer gas decay test. More details on tracer gas testing are given in the occupied home data analysis section of this paper.

In the FRTF, the calculated 15-minute natural infiltration rate was adjusted to include additional duct leakage induced infiltration using tracer gas measurements conducted with and without the central space conditioning system operating. Additional duct leakage induced infiltration was quantified using this method for each stage of the 2-stage 16 SEER heat pump. As the MH Lab has an interior duct system, no duct leakage induced infiltration was included.

Whole house mechanical ventilation (WHMV) was added to each building periodically during the course of experimentation using an unbalanced, continuous point source of supply system. Outside air was introduced directly into the center of the FRTF, and into the utility room of the MH Lab, near the air handler central return. Data collection with and without WHMV was desired as occupied home data collection occurred in homes with and without WHMV operating at ASHRAE 62.2-2010 levels. The WHMV rate was close to ASHRAE 62.2-2010 in each lab building (66 cfm or 31 l/s for FRTF, 57 cfm or 27 l/s for MH Lab). In calculating the total air exchange rate, interactive effects among natural and unbalanced mechanical ventilation were considered using the method described in Appendix C of ASHRAE 62.2-2022.

Lab data was collected from July 2019 to August 2020. Figure 6 shows daily average outdoor dry bulb and dew point temperatures in Cocoa, FL. Consistently high summer dry bulb and dew point temperatures became variable upon the onset of shoulder season at the beginning of November, with variability lasting until the following summer.

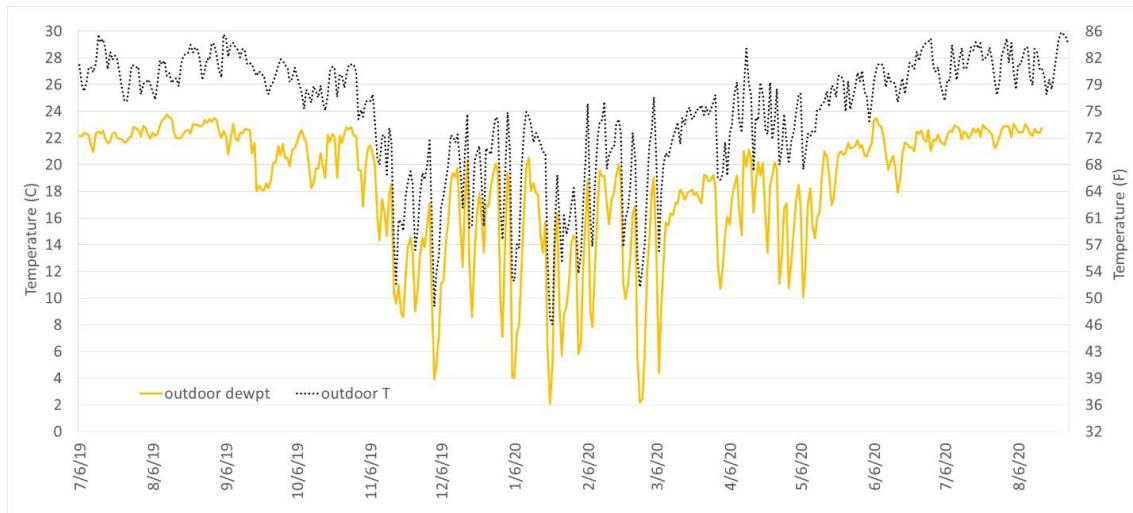


Figure 6. Outdoor dry bulb and dew point temperatures in Cocoa, FL during laboratory data collection.

Figure 7 shows daily FRTF indoor conditions during the data collection period. Consistent mechanical cooling kept indoor temperature constant for much of the year. Some cooling load remains throughout each month of the year, as evidenced by the appreciable condensate collection. During the shoulder season beginning in November, air conditioning becomes less consistent with occasional heating/floating operation resulting from short term cold fronts. As a result, indoor RH becomes more variable. At the beginning of March, the WHMV system was activated, represented by the orange shaded area, resulting in a significant increase in the total air exchange rate, and a significant increase in condensate production. The correlation between infiltration rate and condensate production is evident as the WHMV system was toggled off in June, and back on again in August.

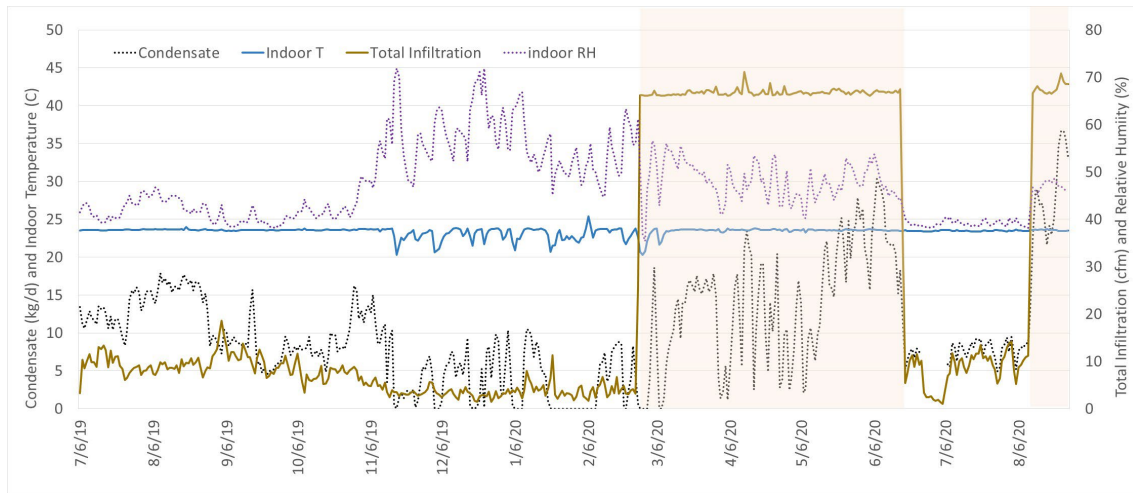


Figure 7. FRTF indoor T and RH, along with measured condensate and calculated total infiltration.

Figure 8 shows actual daily IMG in blue, along with the daily value predicted by the baseline moisture balance model in orange. While data is collected in 15-minute intervals, a daily time step was used for the analysis because the tipping bucket method of condensate quantification is not always accurate at smaller time steps. This is because condensate produced by the air conditioner does not always immediately drain from the system where it can be measured in real time. It is assumed that summing the condensate on a daily basis is representative of the condensate produced that day. Black circles indicate periods of unquantified window condensation affecting the accuracy of prediction.

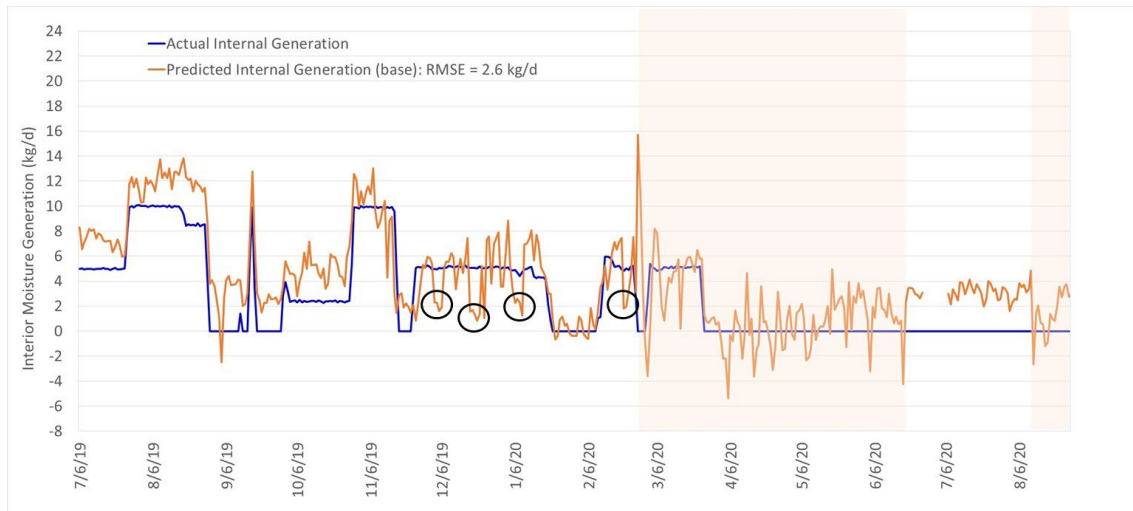


Figure 8. Comparison of actual daily IMG and daily IMG predicted by the baseline moisture balance model.

As seen in Figure 8, the IMG rate was intentionally varied to simulate a range of conditions expected in occupied homes. The COVID-19 pandemic that began in March of 2020 necessitated that researchers work remotely, therefore the internal loads were shut down at that time since the labs could not regularly undergo safety inspections. However, data collection continued. The lab was predominantly operated without WHMV, resulting in relatively low daily average air exchange rates. The WHMV system was operated for periods represented by the orange shaded areas seen in Figure 8.

The overall root mean square error (RMSE) of the prediction over the entire data collection period is 2.6 kg/d (5.7 lb/d). The prediction is consistently biased high during the first summer, indicating an underestimation of moisture sources, or overestimation of moisture sinks. Assuming unexpected measurement error can be ruled out, factors causing the bias may include error in the estimate for natural ventilation rate, and uncertainty regarding the location that the outdoor air infiltrates from. Periodic, short term tracer gas testing confirms reasonableness for estimates of natural ventilation rate,

but the parameter is not directly monitored but rather calculated from monitored T and wind data. While the analysis assumes all of the air came from the outdoors, with conditions indicated by onsite weather station data, a portion may originate from a different location, such as the attic, which at times may contain more moisture than outdoors. The FRTF has a relatively tight ceiling plane however, with no full height interior walls to break up the continuous gypsum air barrier. Moisture diffusion from outdoors or the attic may play a role, with possible vapor drive through the slab, through the un-insulated concrete block walls, or through the ceiling insulated with kraft-faced fiberglass insulation.

The overall prediction improves at the beginning of November 2019 with the onset of swing season, however the prediction gets significantly more variable. At this time of year, with less consistent mechanical cooling, indoor RH becomes highly variable and the need to account for moisture sorption may result in prediction error. While the FRTF is unfurnished, the gypsum drywall, carpet, and exposed slab floor likely play a role in moisture buffering during RH swings. A few events of window condensation on the interior of the single pane windows, indicated by the black circles in Figure 8, result in relatively large errors due to unquantified moisture sinks during condensation and unquantified moisture sources during subsequent re-evaporation. A reasonable prediction is obtained during the relatively few consistent periods of zero condensate collection, indicating that error in the condensate measurement may be a factor.

Average indoor RH is reduced upon the return to consistent mechanical cooling beginning in March 2020, but remains variable due to the activation of the WHMV system. Error in estimating total air exchange rate is expected to be significantly less during WHMV periods since, unlike during natural ventilation periods, the dominant

fan forced component of the total air exchange is measured and monitored directly. The WHMV results in a marked increase in condensate production. While still variable, the average prediction for IMG rate is reasonable during this period, and not biased high like during the initial naturally ventilated summer period, indicating the possibility that the condensate measurement is likely accurate. WHMV was disabled around the middle of June 2020, and re-enabled at the end of the data collection period in August 2020, and similar physical and predicted trends can be observed as in similar previous periods.

### ***Moisture Balance Enhancements to Improve the Accuracy of Prediction***

As stated in the FPL report, moisture balance models mostly differ in terms of how they address the sorption of moisture into and out of building materials and furnishings, a potentially key component to an accurate moisture balance. While it may be justified to neglect sorption if the intent is to model average conditions over long periods (months), when estimating conditions over shorter terms (days, weeks), the effect of sorption can be considerable, if indoor RH (and/or vapor pressure) variations take place. Similar to IMG rate, the effect of sorption is also difficult to measure directly. Boardman and Glass (2015) developed a model that included both short and long term effects for a study investigating the reduction of stack driven moisture infiltration by active soil depressurization. Woods et al. (2014) experimentally determined model inputs on a whole house basis for the effective moisture penetration depth (EMPD) model, which assumes sorption in shallow and deep material layers and is utilized in the US Department of Energy's EnergyPlus building energy simulation program.

During periods with constant indoor RH, one may assume that moisture exchange between the home's air volume and any moisture buffering material in the home is negligible. However, during periods of variable indoor RH, prediction of IMG may be improved via the addition of a moisture buffering term to equation 1.

$$m_z \frac{d\omega_z}{dt} = \dot{m}_{da,v}(\omega_o - \omega_z) + \dot{m}_{g,b} - \dot{m}_c + Ah_m(\omega_s - \omega_z) \quad (3)$$

Rearranging and solving for IMG rate with the buffering term yields:

$$\dot{m}_{g,b} = \dot{m}_c - \dot{m}_{da,v}\omega_o - Ah_m\omega_s + (\dot{m}_{da,v} + Ah_m) \left[ \frac{\omega_z^t - \omega_z^{t-\Delta t} e^{\left(\frac{-\dot{m}_{da,v} + Ah_m}{m_z}\right)\Delta t}}{1 - e^{\left(\frac{-\dot{m}_{da,v} + Ah_m}{m_z}\right)\Delta t}} \right] \quad (4)$$

The moisture buffering term requires knowledge of the whole house buffering material effective surface area, mass transfer coefficient and humidity ratio at buffering material surface. The humidity ratio at the shallow and deep layers of the buffering material were determined using the two-layer effective moisture penetration depth (EMPD) model (Woods and Winkler 2018). The FRTF was one of a few buildings with varying levels of interior furnishings used to experimentally determine whole house based inputs to this model including area of buffering material.(Woods and Winkler 2014). A value of 162 m<sup>2</sup> (1744 ft<sup>2</sup>) for the surface area of buffering material produced a best fit of data for the FRTF, representing a minimally furnished home, while a value of 504 m<sup>2</sup> (5425 ft<sup>2</sup>) produced a best fit in other houses representing average furnished homes. Those values have been used for the buffered model enhancement for the FRTF and MH Lab respectively. Experiments performed by Woods and Winkler (2014) also determined values necessary to estimate the mass transfer coefficient, including depth of shallow and deep layers, slope of the sorption curve, and material vapor permeability. The set of equations used in the EMPD moisture buffering model is summarized in Table 2.

Table 2. EMPD Model Equations for Whole House Moisture Buffering Estimation.

$\dot{m}_{v,s} = \frac{\omega_z - \omega_s}{\frac{1}{h_m} + \frac{\Delta x_s}{2\rho_{air}RT\delta_v}} + \frac{\omega_d - \omega_s}{\frac{\Delta x_s}{2\rho_{air}RT\delta_v} + \frac{\Delta x_d}{2\rho_{air}RT\delta_v}}$	$\dot{m}_{v,d} = \frac{\omega_s - \omega_d}{\frac{\Delta x_s}{2\rho_{air}RT\delta_v} + \frac{\Delta x_d}{2\rho_{air}RT\delta_v}}$
$\varphi_s = \varphi_s^{t-\Delta t} + \frac{\Delta t \cdot \dot{m}_{v,s}}{\rho_m \Delta x_s \frac{du}{d\varphi}}$	$\varphi_d = \varphi_d^{t-\Delta t} + \frac{\Delta t \cdot \dot{m}_{v,d}}{\rho_m \Delta x_d \frac{du}{d\varphi}}$
$\omega = \frac{0.622\varphi P_{sat}}{P_{tot} - \varphi P_{sat}}$	$T_s = \frac{(T_o + T_z)}{2} + \Delta T_s$

The surface temperature of the buffering material is also a required input, however the aforementioned research to determine model inputs obtained surface temperature from within an EnergyPlus simulation. In the case of our research, we intended to apply the moisture balance model to data from a large number of occupied homes, in which the buffering material temperature is unknown, and accurate EnergyPlus simulations for each home are not possible. As a result, the buffering material temperature was estimated from average of indoor and outside air temperature by empirically correcting the difference between this average value and the temperature of the buffering material, as shown in equation (5).

$$T_s = 0.5(T_o + T_z) + \Delta T_s \quad (5)$$

Six temperature correction values ( $\Delta T_s$ ) were determined for a range of indoor and outdoor air temperature differences by minimizing the residual between actual and predicted IMG rate from the base model. Values are shown in Appendix A. EnergyPlus simulations were used to inform the range of values expected for surface temperature of various surfaces contributing to the internal moisture buffering in the FRTF.

While the ability of a moisture buffering focused model enhancement to improve the prediction can be explained in physical terms, the unknown surface temperature and resulting empirical determination based on an optimized fit of the

model to the data suggests that the resulting correction could also account for any of the previously discussed sources of error, as well as any difference in the rate by which the model responds to moisture sources/sinks vs. various lags that likely exist in the physical building. Therefore, a second model enhancement, shown by equation (6) was investigated using a linear model approach to correcting errors in significant measured and estimated quantities including indoor and outdoor humidity ratio, condensate, and ventilation rate. Coefficients of equation (7) were determined through regression of the moisture generation residual between the actual and predicted values determined by the base model, and are shown in Appendix A.

$$\dot{m}_{g,b} = \dot{m}_g + \Delta\dot{m}_{g,c} \quad (6)$$

$$\Delta\dot{m}_{g,c} = g_0 + g_1\omega_o + g_2\omega_z + g_3\dot{m}_{da,v} + g_4\dot{m}_c + g_5\dot{m}_{da,v}\omega_o \quad (7)$$

Figure 9 shows how both the moisture buffering based model enhancement, shown in yellow, and the linear model correction based enhancement, shown in light blue, improve the prediction of the base model shown in green. Both model enhancements result in similar prediction improvement with the RMSE for the buffering and linear correction enhancements 1.8 and 1.7 kg/d (4.0 and 3.7 lb/d) respectively, compared to the 2.6 kg/d (5.7 lb/d) obtained with the base model.

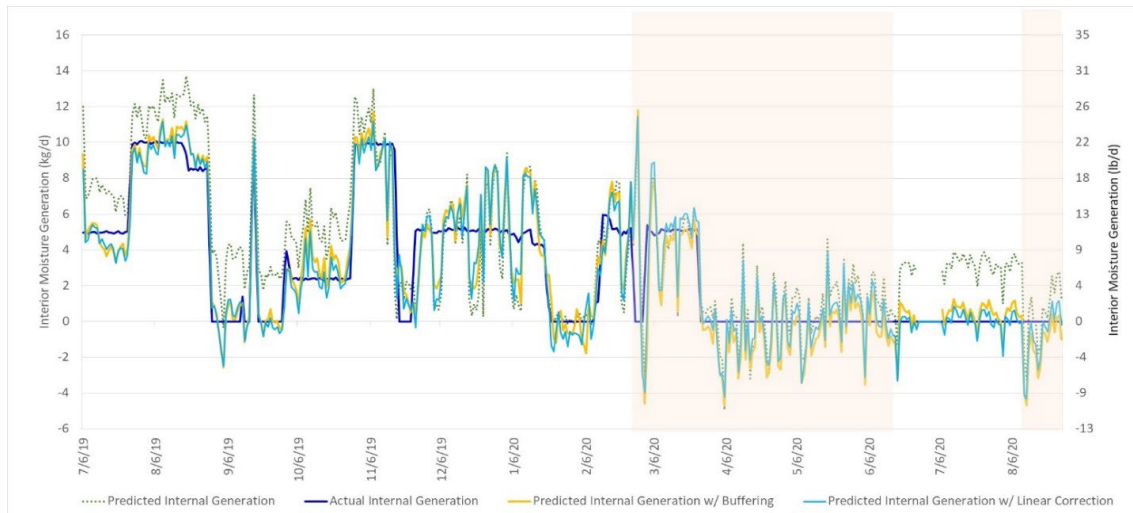


Figure 9. Improved predictions of the moisture buffering based enhancement (yellow) and the linear model based correction (light blue), over the baseline moisture balance model (green).

Additional model enhancements were considered to potentially account for, in physical terms, the over-prediction of IMG by the baseline moisture balance model during the first and second summer. During these periods, indoor RH is relatively constant, indicating that moisture buffering flux is likely negligible. During these periods, outdoor moisture content is high, and an underestimation of natural ventilation rate could result in the over-prediction of IMG. Models that applied a consistent correction factor to natural ventilation rates throughout the entire data collection period were developed, resulting in the desired summertime prediction improvement with negligible impact prediction accuracy during times of the year with lower outdoor moisture content. However, there was no definitive justification for applying a correction factor to the calculated natural ventilation rates, which were spot checked with tracer gas testing.

To arrive at the desired correction, consideration of moisture diffusion was added to the baseline model, considering diffusion through both the wall and the ceiling,

shown in equation (8). While the effect of moisture buffering may be negligible during the summer months, it may be significant during times of the year with variable indoor RH, and therefore was also added to the diffusion enhanced model. The equation formulation was also changed from humidity ratio to vapor density.

$$V_z \frac{dc_z}{dt} = \dot{V}_V(c_o - c_z) + \dot{m}_g - \dot{m}_c + A\bar{h}_{buff}(c_s - c_z) + A\bar{h}_{ceil}(c_o - c_z) + A\bar{h}_{wall}(c_o - c_z) \quad (8)$$

The difference between indoor and outdoor conditions are utilized to estimate moisture diffusion flux through both the walls and the ceiling. Attic conditions were not monitored in the occupied homes, and daily average attic moisture conditions are closely approximated by daily average outdoor moisture conditions in vented attics. An analytical solution solving for IMG is included in Appendix B, and yields:

$$\dot{m}_g = \dot{m}_c - \dot{V}_V c_o - A\bar{h}_{ceil} c_o - A\bar{h}_{wall} c_o + (\dot{V}_V + A\bar{h}_{ceil} + A\bar{h}_{wall}) \left[ \frac{c_z^t - c_z^{t-\Delta t} e^{\left(-\frac{\dot{V}_V + A\bar{h}_{ceil} + A\bar{h}_{wall}}{V_z}\right)\Delta t}}{1 - e^{\left(-\frac{\dot{V}_V + A\bar{h}_{ceil} + A\bar{h}_{wall}}{V_z}\right)\Delta t}} \right] \quad (9)$$

To determine vapor transfer coefficients for the diffusion and buffering terms, EnergyPlus combined Heat and Moisture Transfer (HAMT) algorithm was used to inform us on the range of vapor transfer coefficient values anticipated. EnergyPlus source code was modified to add vapor transfer coefficients report variable for the HAMT model. The vapor transfer coefficients in the steady state vapor diffusion model through the assemblies were determined from layer-by-layer combination of vapor diffusion coefficients of the material layers of the assembly construction for each surface type and the air films on both sides the surfaces. The diffusion coefficients through each of the construction layers were determined from vapor permeability

assumed for each of the materials of construction. Constant vapor diffusion coefficients were assumed for the air films on both sides of the surfaces.

One of the challenges of working with buffering enhanced moisture balance models has been determining buffering material moisture content. In the previous formulation, the EMPD model was utilized, which required knowledge of buffering material surface temperature, which had to be estimated. In this new formulation, moisture content of the buffering material was investigated by estimating the vapor density at buffering material surface using a linear model.

Rearranging the above equation enables the calculation of surface vapor density using the laboratory's known IMG rate. In order to utilize the moisture balance with data from occupied homes with unknown IMG rates, the calculated vapor density was fit to a linear model as a function of variables monitored/measured in both the lab homes and occupied homes. Detailed and simple linear model equations for predicting vapor density at the buffering material surface were formulated and investigated, and discussed more in Appendix B. Ultimately, the simple model was utilized that expressed surface vapor density as a function of indoor and outdoor moisture:

$$c_s = a_0 + a_1 \dot{V}_V c_o + a_2 c_z + a_3 c_o \quad (10)$$

Figure 10 shows how the moisture balance model with the added diffusion enhancement, shown in black, results in an improved RMSE of 2.1 kg/d (4.6 lb/d) compared to the baseline model shown in orange. Adding the newer surface vapor density moisture buffering formulation, shown in red, improves the RMSE of the prediction to 1.7 kg/d (3.7 lb/d), which is similar to the previous linear correction enhancement.

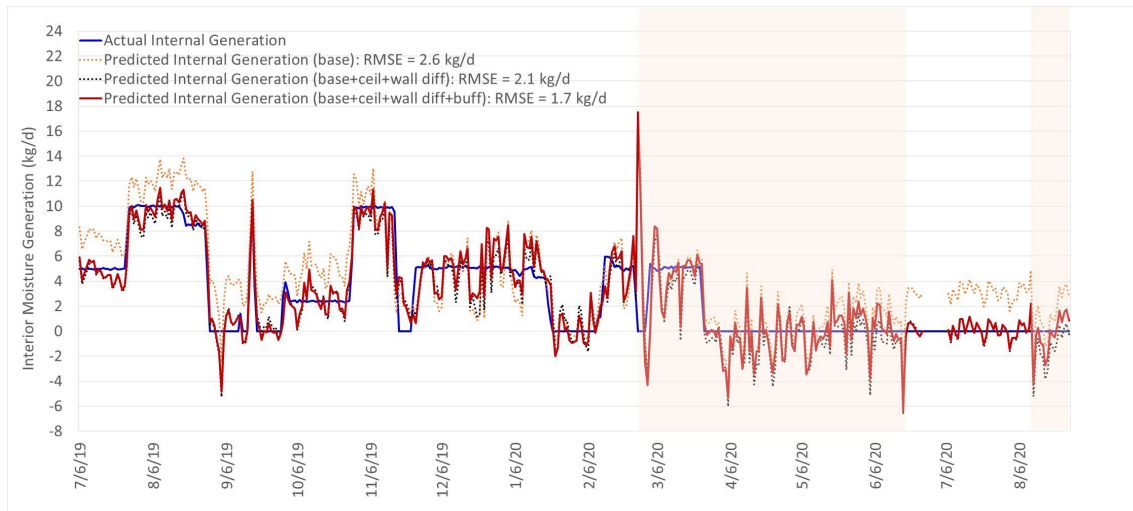


Figure 10. The prediction of the diffusion enhanced baseline model (black) in the FRTF is further improved over the baseline model (orange) with the addition of the new surface vapor density moisture buffering formulation (red).

On average the relative errors obtained are reasonable considering long term data collection. However in consideration of application of a final model to occupied home data, for this particular research only six days of data are available for each home (further discussion of the occupied home data collection protocol is included in the next section). Over such a short term, model prediction may be poor, depending on a number of factors including season, whether the home is naturally or mechanically ventilated, etc. Therefore, RMSE was evaluated using six-day averages of daily IMG to see if it improved over results obtained with daily data. Results of the six-day averaging are shown in Figure 11. The overall RMSE for the model with diffusion and buffering improves slightly to 1.3 kg/d (2.9 lb/d). However, the six day averaging significantly smooths out the magnitude of short term variability of prediction accuracy under certain conditions. This indicates that, when applied to short term data from occupied homes, IMG predicted for an individual day could have a relatively large error ( $> \pm 5$  kg/d, 11 lb/d), but the 6-day average IMG is likely to be able to be predicted with reasonable

accuracy. RMSE was also evaluated by running the models with six-day averages of all independent input variables, and results were found to almost identical to those obtained by averaging the daily calculated IMG rate.

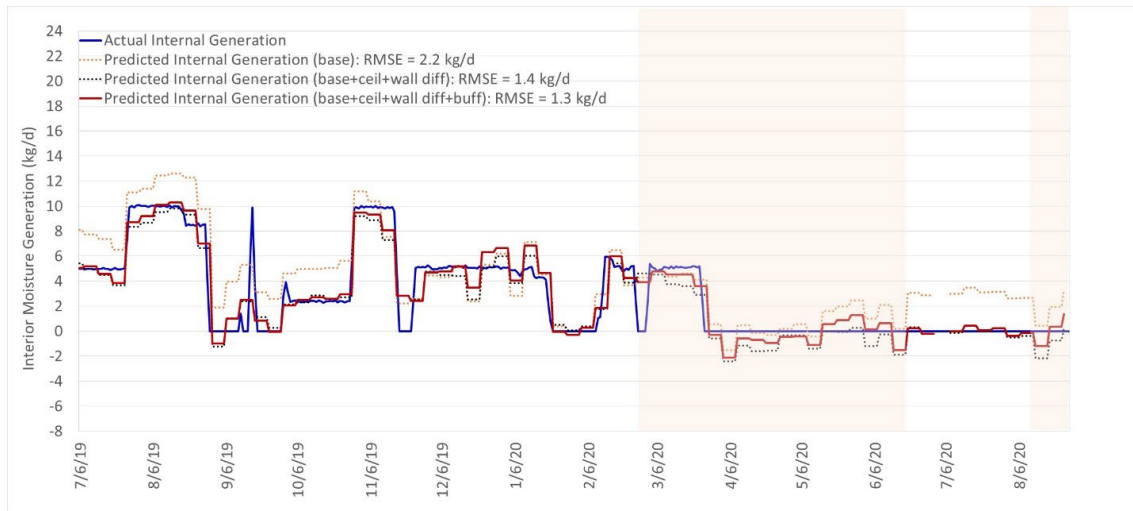


Figure 11. Model results when 6-day averages of input data are applied from the FRTF.

#### *Application of the Moisture Balance and Enhancements to Data from the MH Lab*

The diffusion enhanced moisture balance was applied to data from the MH Lab collected between September 2019 and July 2020 to determine how the accuracy of the predictions may change when the approach is applied to a different building: in this case a lower mass, less air tight, more heavily furnished home with multiple spaces. For the MH Lab, diffusion through the walls was considered negligible due to the vinyl exterior cladding, and vapor retarding wall sheathing and insulation. However, a diffusion term for the crawlspace floor was added. As with most manufactured homes, the MH Lab does have a vapor barrier “belly board” under the floor, however the integrity has deteriorated over time. Monitored conditions in the crawlspace and inside the belly of the home were utilized as inputs to the diffusion terms in the model. Figure 12 shows the results for the base model in orange with an RMSE over the period of 8.4 kg/d (18.5 lb/d). It was later discovered that air conditioning condensate had been pooling inside

the crawlspace, with diffusion through the floor resulting in a large source of error during summer months. The model that considers both diffusion and buffering (red) reduces the RMSE to 3.0 kg/d (6.6 lb/d).

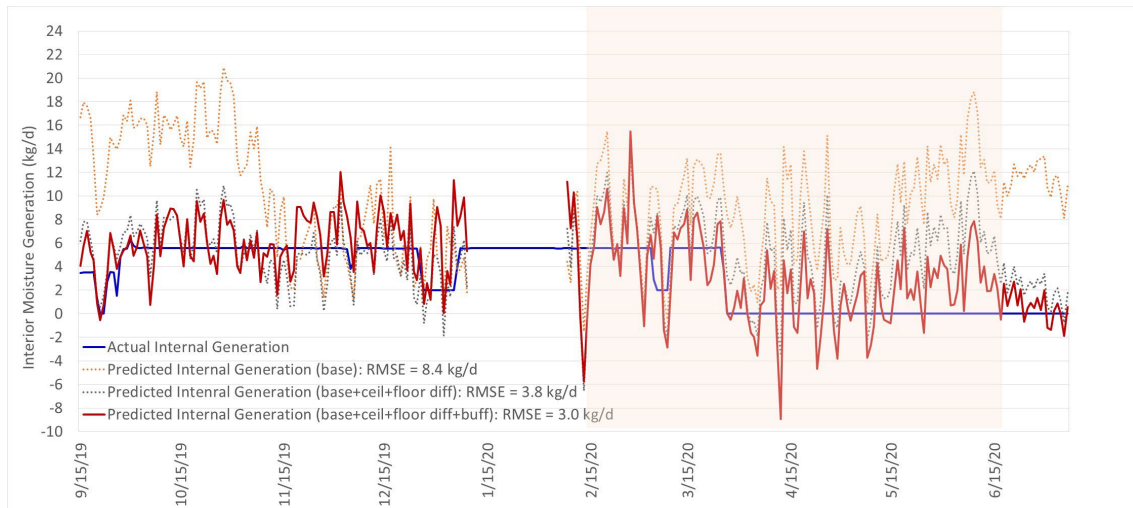


Figure 12. The prediction of the diffusion enhanced baseline model (black) in the MH Lab is further improved over the baseline model (orange) with the addition of the new surface vapor density moisture buffering formulation (red).

The models result in a more variable prediction than in the FRTF, presumably due to additional error in calculating natural infiltration rates in this leakier building.

Figure 13 shows that the 6-day averaging increases the accuracy of prediction with an RMSE of 1.9 kg/d (4.2 lb/d).

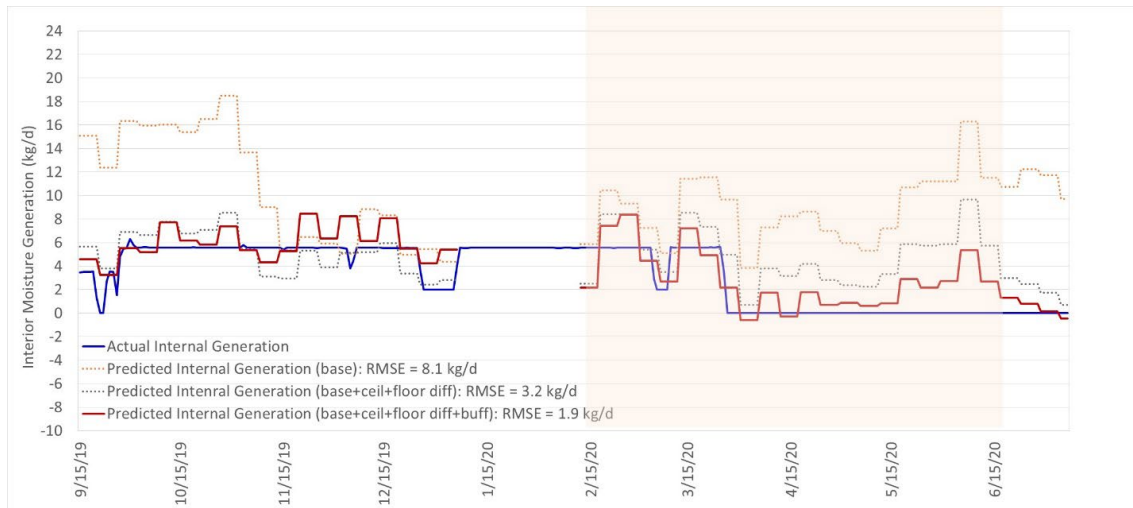


Figure 13. Model results when 6-day averages of input data are applied from the MH Lab.

*Application of the moisture balance to other buildings with unknown parameters*

While RMSE for the moisture balance model with enhancements is reasonable when coefficients can be determined with an empirical fit of the models to known IMG rates, the ultimate intent of this research is to validate a model that can be applied to data from occupied homes with unknown IMG rates. Therefore, the resulting models with coefficients empirically determined for one lab were applied to the data from the other lab. Figure 14 shows the result of applying the MH Lab buffering model coefficients to data from the FRTF. Resulting RMSE increases slightly to 1.9 kg/d (4.2 lb/d), up from a value of 1.3 kg/d (2.9 lb/d).

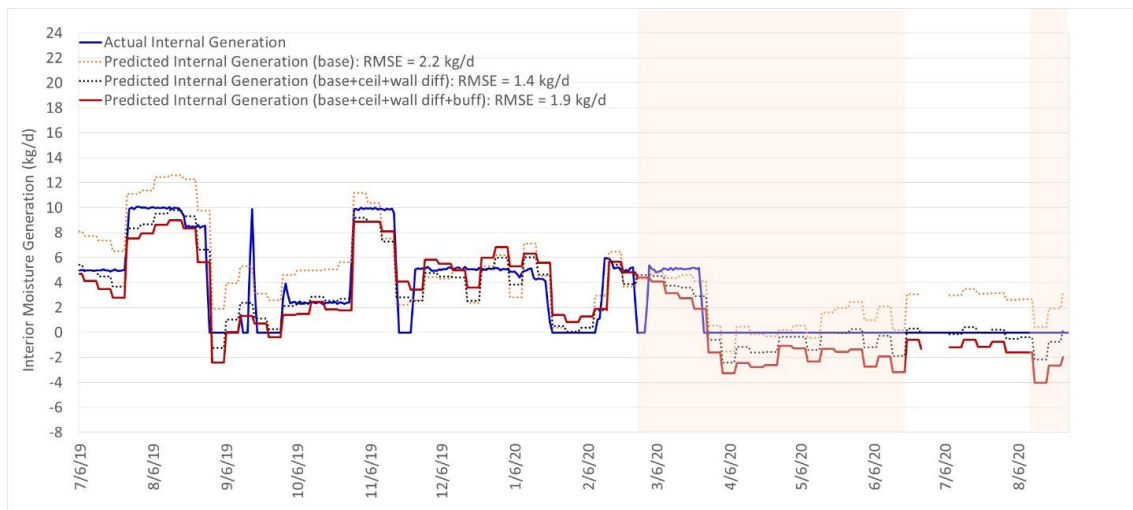


Figure 14. Model results when MH Lab buffering model coefficients are applied to data from the FRTF.

## Application of the Moisture Balance Model to Occupied Home Data

### *Home Recruitment*

FSEC developed a recruitment strategy and targeted a diverse mix of homes that reflect the general characteristics of newer housing in the warm humid climate region. FSEC's energy rated homes database served as the primary source of records to identify homes that met study requirements for recruiting purposes. The database contains detailed information on homes that have undergone an energy audit for which FSEC has performed quality control and archived the results. A similar database maintained by RESNET was used as a secondary source of records. The databases include the address of the home, year of construction, and detailed information on physical characteristics of the home and mechanical systems. The databases do not contain any homeowner contact information or other personally identifiable information. As it is more common for homes that have been built better than code to obtain an energy audit, the databases contain significantly more above-code homes than minimum-code homes.

The main outreach method for recruitment was postcards that were sent to homes identified from the pre-existing databases as meeting the general criteria of being built since 2013 in the states of Florida, Georgia, and South Carolina. The postcards directed interested persons to either contact FSEC by phone or email or visit a project website to obtain more information. Homeowners were offered compensation in the form of home improvement store gift cards for their participation. A report summarizing data collected from each home was also provided.

### ***Home Characterization***

A total of 51 homes were recruited and participated in the BIAAQ study. Forty homes were located in FL, six in SC, and five in GA. This paper includes estimates for IMG in 30 of those homes, 23 of which were located in FL, five in SC, and two in GA. Figure 15 shows the geographic distribution of the homes. Recruitment and data collection began in September 2018 and was started/stopped a few different times as a result of the COVID-19 pandemic. Data collection ended in March 2022.

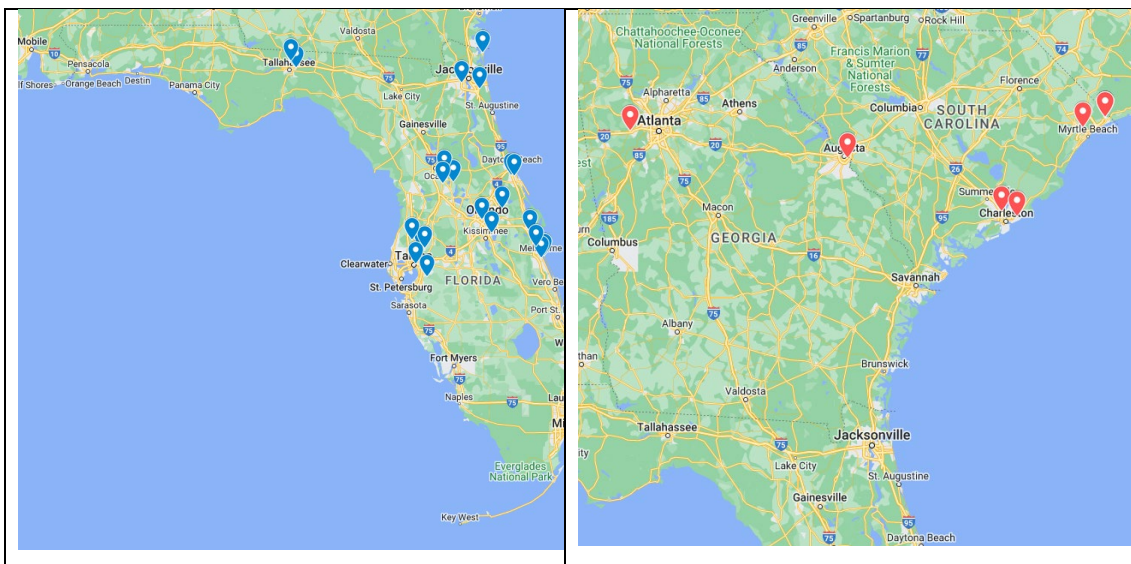


Figure 15. Geographic distribution of homes.

Table 3 provides a summary of the conditioned area, year of construction, and full-time occupancy for the recruited homes. All homes were single-family detached, and all foundations were slab on grade with the exception of one slab/stem wall home in SC. Twenty two homes were single story and eight homes were two-story. Additional data for each home is shown in Appendix C.

Table 3. Summary of home and occupancy characteristics.

<b>Characteristic</b>	<b>Median</b>	<b>Range</b>
Conditioned Area, m <sup>2</sup> (ft <sup>2</sup> )	185 (1985)	112-360 (1205-3869) <sup>a</sup>
Year Built	2017	2014-2020
Number of Occupants	3	1-6

<sup>a</sup> Only homes less than 372 m<sup>2</sup> (4,000 ft<sup>2</sup>) and greater than 84 m<sup>2</sup> (900 ft<sup>2</sup>) were targeted.

### ***Whole House Mechanical Ventilation System (WHMV) Characterization***

Homes with WHMV systems for which source records indicated met the minimum requirements of ASHRAE 62.2-2010 were targeted for recruitment. This version of the standard was chosen as the benchmark for this study as it is the version required by code and above-code programs for homes in the southeastern US region, and it is difficult to find a significant number of homes with systems that meet minimum requirements of more recent versions of the standard. As described in Martin et al. (2020) many of the WHMV systems were found to be non-operational. Problems encountered included failed dampers, disconnected wiring, and maintenance issues. For the systems that were found to be operational, the vast majority were not operating upon arrival, or operating well below design. In certain homes, the study team obtained permission from the occupants to operate the WHMV system during all or part of the data collection period.

The most common approach found for providing WHMV was via an exhaust fan (EXH). All exhaust WHMV fans encountered were installed in bathrooms, and also

designed for spot exhaust purposes. While most exhaust fans had simple on/off switches, a small number of systems had controls located in a switch that enabled the fan to operate intermittently based on an adjustable time setting, and achieve a minimum hourly runtime. Such controls often also enabled the fans to be operated based on indoor humidity and/or occupancy, either independently from, or in addition to, the time setting. The second most common WHMV system type encountered were central fan integrated supply (CFIS) systems that were configured to use the home's central forced air heating and cooling system to temper and distribute outdoor air that is pulled in through a ducted connection from outside to the return side of the forced air system. This supply-based WHMV system is typically set up to pull outdoor air through the system using the negative return side pressure generated when the forced air system fan operates. Passive CFIS systems that are "uncontrolled" rely exclusively on the heating/cooling runtime of the forced air system and thus are not ASHRAE 62.2 compliant. Some manufacturers package control and damper systems that invoke additional air handler fan runtime to meet flow targets on an hourly basis. These "controlled" CFIS systems may be programmed via a thermostat or a separate controller that connects to the thermostat

A limited number of balanced ventilation systems were encountered that combine supply and exhaust fans that are set to operate in unison, balancing pressure between indoors and outdoors. All such systems encountered were energy recovery ventilators (ERV) that enable both heat and moisture to be transferred between incoming and outgoing air streams to retain some of the energy used to condition the indoor air. A limited number of ventilating dehumidifiers (DEHU) were encountered that delivered outside air into the return duct system of the central heating and cooling system. The systems deliver outside air via their own fixed capacity fans, and operate

independently of the central heating and cooling system, with programming that enables them to operate intermittently and deliver a target hourly ventilation rate. Most systems were not configured with capability to dehumidify the main living space, and did not have a return duct from the space. The dehumidifier compressor operated based on a customizable humidity set point, but only removed moisture from the outdoor air stream when the humidity in the main living space exceeds the set point during ventilation operation.

### ***Occupied Home Data Collection Methodology***

The occupied home data collection protocol used for the BAI AQ study, and leveraged for ASHRAE RP-1844, was modelled after an earlier study called the Healthy, Efficient, New Gas Homes study (Chan, 2020) that was conducted by the Lawrence Berkeley National Laboratory and collected data in CA representing mixed dry climates. The description of the field measurement protocol that follows is not representative of the entire BAI AQ protocol, and only focuses on measurements/activities related to estimating IMG rates.

Each study home was visited multiple times by a two-person field team. On the first visit, the field team:

- Explained the study intent and requirements and obtained written consent from participants.
- Completed house and heating, cooling, and ventilation system characterization.
- Installed devices to measure environmental conditions indoors and outdoors, and installed devices to monitor heating/cooling system operation, and use/operation of home features and equipment that affect air exchange with the outdoors

including WMHV systems, kitchen, bath, and laundry exhaust for spot ventilation, clothes dryers, and exterior doors.

Participants were asked to partake in normal household activities with the exception that windows and doors should not be used for natural ventilation during the data collection period. Most homes were monitored for one week – some with an operating WHMV system, some without. During the final field team visit, all data collection devices were removed, and tests were conducted to quantify airflow of air moving equipment, and to characterize building envelope and duct leakage.

Temperature and relative humidity were measured outdoors, and in various locations inside the home. Table 4 describes measurement equipment, and sampling locations in each home. Wind speed was obtained from the National Weather Service monitoring site geographically closest each home.

Table 4. Instrumentation for temperature and relative humidity measurements.

<b>Location</b>	<b>Resolution</b>	<b>Measurement Device</b>	<b>Accuracy</b>
Outdoors, Master Bathroom, Second Bathroom, Kitchen	1 minute	Onset HOBO U23 Pro v2	0.2°C / 2.5% RH
Central Indoors, Master Bedroom, Second Common Area	1 minute	AirVisual Pro	0.2°C / 2.5% RH

Runtime of equipment that affects air exchange with the outdoors was monitored utilizing instruments listed in Table 5. The position (open or closed) of patio and garage-to-house door, along with the door to the master bedroom, was also monitored. Condensate produced by air conditioning and dehumidification systems was collected and quantified by modifying the condensate drain line outside of the home to drain into a tipping bucket.

Table 5. Instrumentation for equipment runtime, door status, and condensate production.

<b>Parameter</b>	<b>Measurement Device</b>
WHMV system operation	Digisense anemometer WD-20250-22
	Onset plug load logger UX120-018
Master/second bathroom exhaust fan operation, Range hood operation	Digisense anemometer WD-20250-22
Clothes dryer operation	Onset motor on/off logger UX90-004 (electric)
	Onset plug load logger UX120-018 (gas)
Forced air system runtime– supply (up to two zones)	Digisense anemometer WD-20250-22
	Onset HOBO UX100-003 T/RH
Patio door, garage-to-house, master bedroom door status	Onset state sensor UX90-001
Air conditioner / dehumidifier condensate	Texas Instruments tipping bucket

A one-time measurement to quantify air flow generated by all equipment generating fan forced air flows into and out of the home was conducted. Devices utilized for these measurements included a powered flow hood, an exhaust fan flow meter, and a duct blaster. Except in the case of a few WHMV systems integrated with multi- or variable speed heat pumps, all fan flows deliver a constant amount of airflow during operation, and therefore a single airflow measurement was sufficient for flow characterization.

### ***Determining Outdoor Air Exchange***

Daily average total air exchange was calculated by combining calculated hourly natural infiltration and measured/monitored fan forced ventilation flows according to the method found in Appendix C of ASHRAE Standard 62.2-2022 (ASHRAE 2022), considering interactive effects among unbalanced flows, and rolling up to daily values. To determine inputs and coefficients for the natural infiltration model, a Delta-Q test (Walker, Dickerhoff, and Sherman 2002)) was conducted in each home to measure building envelope and duct leakage, and determine envelope leakage flow coefficient and exponent. In most homes, short term tracer gas testing with SF<sub>6</sub> was also conducted to yield a secondary measure of infiltration resulting from envelope leakage and duct leakage. Some occupants chose to opt-out of this testing. In other homes, time constraints or instrument issues prevented the tracer gas test from being conducted. The tracer gas decay test (ASTM 2017) was performed over the course of approximately one and one half hours. At the start of the test SF<sub>6</sub> was injected with the central space conditioning operating to aid in mixing. Maximum concentrations of no more than 1 ppm of SF<sub>6</sub> were targeted as a safety precaution. Concentrations were sampled at multiple locations throughout the house and once concentration was determined to be well mixed, the SF<sub>6</sub> concentration decay was recorded approximately every 10 minutes. After approximately 40 minutes of measurements with the central space conditioning system operating, another 40 minutes of measurements were collected with the central space conditioning system “off”. Typically tracer gas decay tests are conducted over a minimum of one complete air change. However, the length of time spent inside the homes carrying out the entire data collection protocol limited the amount of time available for tracer gas testing. As mentioned, the testing was conducted for two operating conditions, typically with central space conditioning system “on” and “off”,

yielding snap-shot estimates of natural infiltration, and additional infiltration resulting from duct leakage. In some instances, one or both of the operating conditions may have included an operating WHMV system, depending on how the home operated during the data collection periods.

As with the lab homes, the flow coefficient and exponent obtained from the Delta Q test were used along with monitored indoor/outdoor temperatures and wind speed to calculate the wind and stack-driven components of natural infiltration using the ASHRAE enhanced model procedure found in Appendix C of ASHRAE Standard 62.2-2022 (ASHRAE 2022). For homes with tracer gas results, a non-linear solving method was used to calibrate the natural infiltration model coefficients so that the calculated natural infiltration rate during the test aligned with measured result obtained during the test. For homes without tracer gas results, the default model coefficients were used. Figure 16 shows how calculated natural infiltration in one home obtained with coefficients derived from tracer gas testing compares to calculated natural infiltration rates with default model coefficients. Figure 17 compares natural infiltration obtained during tracer gas testing with calculated natural infiltration rates for the same time period.

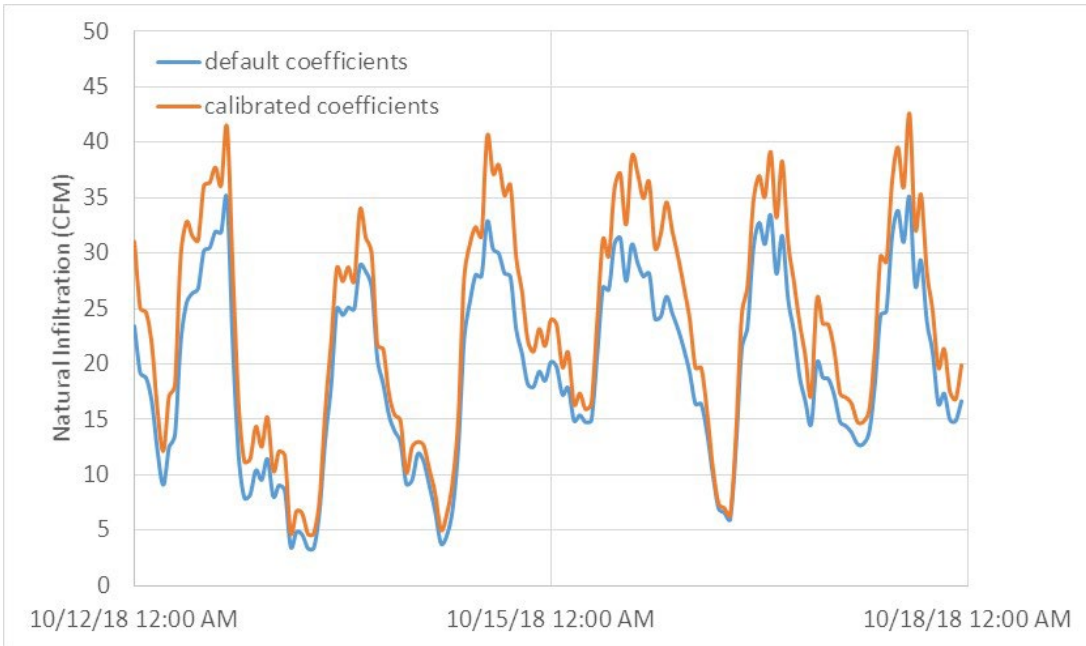


Figure 16. Comparison of calculated natural infiltration using default model coefficients and coefficients calibrated through the use of tracer gas testing.

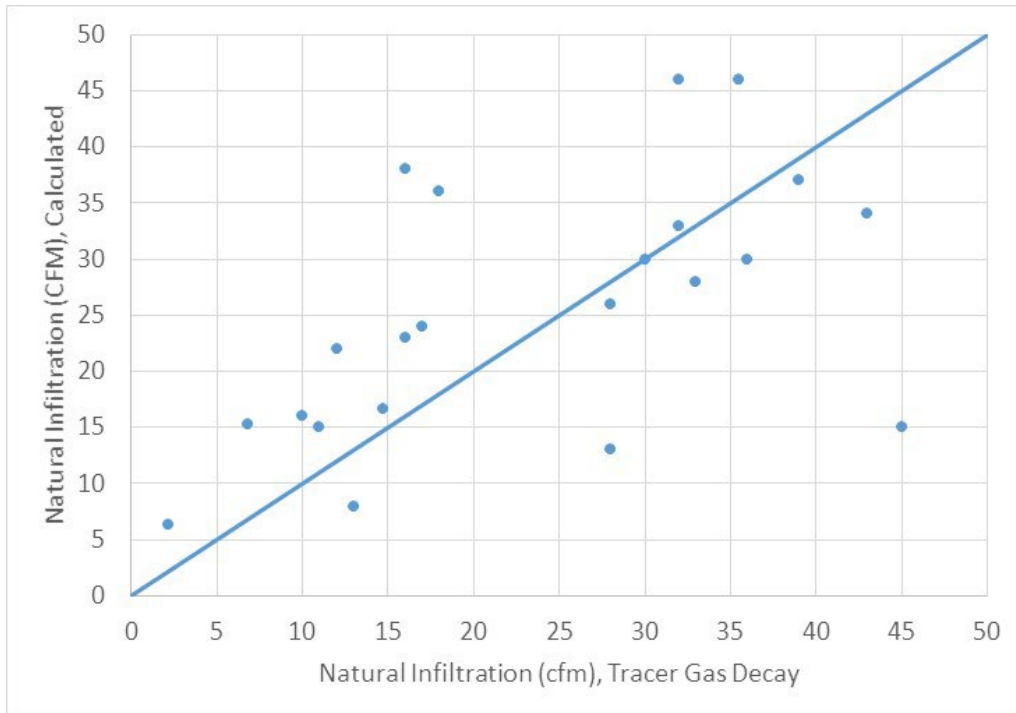


Figure 17. Comparison of natural infiltration obtained with tracer gas testing and obtained via calculation.

In many homes, tracer gas testing results were also used as a secondary measure of duct leakage to outdoors. For homes where Delta Q results indicated a supply or return duct leakage as dominant, the infiltration obtained from tracer gas testing while the space conditioning system was “on” was used to represent duct leakage to outdoors. For homes where Delta Q results indicated balanced duct leakage on the supply and return side, the difference in infiltration obtained from tracer gas testing while the space conditioning system was “on” and “off” was used to represent duct leakage to outdoors. For homes that did not undergo tracer gas testing, or tracer gas testing involved operation of a WHMV system, Delta Q duct leakage values were used. Select homes had ducts located within a conditioned attic, in which case zero duct leakage to outdoors was assumed.

### ***Application of Moisture Buffering Model Enhancements to Occupied Home Data***

Data collected from each occupied home was processed and input into the baseline moisture balance model. The diffusion enhancement was applied to account for diffusion through ceilings under vented attics only. As all homes were slab-on-grade, no floor diffusion was modelled. All homes were of newer construction with sufficient vapor resistance from exterior claddings and insulation in the wall assembly, therefore no wall diffusion was modelled. The moisture buffering enhancement was applied to homes with a swing in daily average indoor RH greater than 5% during the data collection period, utilizing coefficients derived from the MH Lab. The area of whole-house buffering material (m<sup>2</sup>) was estimated to be 1.3 times the house air volume (m<sup>3</sup>), which was a typical ratio found in test buildings used by Woods and Winkler (2018). In a sensitivity analysis of inputs to the EMPD model, Woods and Winkler 2018 found that of all moisture buffering material, drywall played the largest role in overall

moisture buffering. Experimental homes utilized to assess the model's ability to predict indoor RH had drywall area to volume ratios of approximately 1.3.

## **Results and Discussion**

Results are shown in Tables 6 and 7, and include the calculated IMG rate for each day of the 6-day testing period, and the average rate for the period. Also included is the ASHRAE Standard 160-2021 guidance, based on the number of occupants, and the ANSI/RESNET/ICC Standard 301 values, based on the conditioned floor area and the number of bedrooms. As seen in the results tables, IMG varies from day to day, as expected, likely resulting from occupancy and occupant behavior. The number of full-time occupants in each home is listed in the tables, however, there are daily variations in occupancy during the data collection period. These occupancy variations can explain some variations in daily IMG rates. For example, in home 402, the homeowners reported having a party on Day 2, likely accounting for the higher daily generation rate. Similarly, for home 414, the homeowners reported having a party and overnight guests on Days 4 and 5. There are a number of instances of zero daily IMG in the tables. The calculated result for these days are often slightly negative, but have been truncated to zero in the tables as negative IMG is not possible. These low daily values may be explained by lower than average occupancy/activity, or possibly condensate measurement error. Accuracy of condensate collection for occupied homes may occasionally be lower than experienced in the lab homes. While the lab home tipping buckets are permanently installed, the tipping buckets for the occupied homes needed to be custom installed and levelled at each home, and the potential exists for them to be accidentally clogged or bumped by homeowners, pets, etc.

Table 6. Calculated IMG rates (SI units)

Home #	Internal Moisture Generation (kg/d)							ASHRAE 160, 70th Percentile Value	ANSI / RESNET Value	Number of People/ bedrooms	Data Collection Month	Average Daily Condensate (kg/d)	Average Indoor RH (%)	Average Outdoor RH (%)	Average Outdoor Dew Point (C)	WHV Type	ACH50	Floor Area (m <sup>2</sup> )
	Day #						Avg											
	1	2	3	4	5	6												
402	11	16	7	8	11	11	10	9	5	3/3	Oct	24	49.9	77.0	23.9	None	2.9	248
403	9	6	6	6	3	7	6	10	5	4/3	Oct	20	54.9	78.2	22.8	None	4.1	196
405 <sup>a</sup>	4	2	4	17	5	1	5	9	5	3/3	Nov	8	62.6	76.7	14.3	ERV	3.7	191
408	2	0	13	12	12	2	7	9	7	3/4	Dec	0	54.2	87.6	9.7	None	1.7	293
409	4	13	9	3	6	8	7	7	5	2/3	Jan	0	55.6	75.4	7.6	None	5.4	183
410	5	2	4	6	6	3	5	7	9	2/5	Jan/Feb	0	54.4	69.9	6.5	None	1.8	360
411	9	7	9	6	6	8	8	12	7	6/4	Feb	9	60.8	71.4	15.7	None	4.0	149
414	7	8	10	19	17	15	13	10	7	4/4	Feb/Mar	21	53.7	83.5	17.2	Dehu	2.3	270
415	0	6	8	9	16	8	8	11	5	5/3	Mar	5	58.8	75.2	11.6	ERV	4.8	112
416	5	3	3	5	3	5	4	7	5	2/3	Mar	6	59.4	68.4	14.8	ERV	4.3	1724
418 <sup>a</sup>	13	18	7	5	4	10	10	11	9	5/5	Mar/Apr	16	56.8	70.6	15.8	ERV	3.6	289
420 <sup>a</sup>	15	8	10	13	12	9	11	11	7	5/4	Apr	19	54.8	66.5	14.6	Dehu	2.0	281
421	5	0	11	4	8	5	5	7	5	2/3	Apr	11	55.6	60.9	17.2	CFIS	4.5	124
422	8	7	4	1	4	4	5	7	5	2/3	Jul	12	60.2	70.5	23.8	CFIS	5.5	112
424	9	4	10	11	10	6	8	7	5	2/3	Aug	20	58.6	84.9	24.8	None	5.9	165
425	5	2	4	3	2	1	3	9	5	3/3	Aug	25	55.8	78.4	23.9	None	3.5	170
427	3	4	5	5	4	6	5	7	5	2/3	Sep	6	44.4	49.8	13.9	None	4.0	179
430	0	2	7	0	4	3	3	9	5	3/3	Oct	9	58.8	84.3	18.8	None	5.7	167
431	17	5	4	11	0	0	6	11	7	5/4	Dec	3	56.2	75.4	10.0	None	3.2	277
432 <sup>a</sup>	11	10	14	0	0	19	9	9	5	3/3	Dec	2	51.9	79.6	8.8	EXH	3.7	205
435	16	13	4	3	7	4	8	9	5	3/3	Nov	2	60.8	75.3	13.8	None	3.9	170
437	0	5	15	8	2	5	6	9	7	3/4	Dec	0	68.3	79.2	12.6	None	3.3	236
440	10	14	10	4	3	4	8	9	9	3/5	May	17	52.0	60.9	17.2	None	3.9	328
441	9	4	1	0	6	2	4	7	7	2/4	May	15	48.2	64.5	18.5	None	4.3	240
442	0	7	7	1	0	0	3	7	5	2/3	Jun	29	58.3	72.5	21.4	Exh	4.1	141
443	6	11	10	1	4	1	5	7	5	2/4	Jun	29	62.4	68.5	21.4	Exh	5.9	149
444	7	7	2	9	12	6	7	7	5	2/3	Jul	12	60.2	71.2	19.6	None	4.7	160
445 <sup>a</sup>	4	6	0	0	0	7	3	10	5	4/3	Jul	22	59.3	81.8	23.1	EXH	4.8	153
446 <sup>a</sup>	0	4	0	4	6		3	7	5	1/3	Aug	13	52.3	87.9	24.8	None	5.0	151
447 <sup>a</sup>	8	9	8	4	3	0	5	9	7	3/4	Sep	21	54.6	81.3	23.3	None	4.8	213

<sup>a</sup>Default coefficients used for natural infiltration model rather than coefficients calibrated with tracer gas results.

Table 7. Calculated IMG rates (IP units).

Home #	Internal Moisture Generation (lb/d)							ASHRAE 160, 70th Percentile Value	ANSI / RESNET Value	Number of People/ bedrooms	Data Collection Month	Daily Average Condensate (lb/d)	Average Indoor RH (%)	Average Outdoor RH (%)	Average Outdoor Dew Point (F)	WHV Type	ACH50	Floor Area (ft <sup>2</sup> )
	Day #						Avg											
	1	2	3	4	5	6												
402	24	35	15	18	24	24	23	20	12	3/3	Oct	53	49.9	77.0	75.0	None	2.9	2670
403	20	13	13	13	7	15	14	22	12	4/3	Oct	44	54.9	78.2	73.0	None	4.1	2104
405 <sup>a</sup>	9	4	9	37	11	2	12	20	12	3/3	Nov	18	62.6	76.7	57.7	ERV	3.7	2055
408	4	0	29	26	26	4	15	20	16	3/4	Dec	0	54.2	87.6	49.5	None	1.7	3150
409	9	29	20	7	13	18	16	15	12	2/3	Jan	0	55.6	75.4	45.7	None	5.4	1967
410	11	4	9	13	13	7	10	15	19	2/5	Jan/Feb	0	54.4	69.9	43.7	None	1.8	3869
411	20	15	20	13	13	18	17	26	15	6/4	Feb	20	60.8	71.4	60.3	None	4.0	1597
414	15	18	22	42	37	33	28	22	16	4/4	Feb/Mar	46	53.7	83.5	63.0	Dehu	2.3	2900
415	0	13	18	20	35	18	17	24	12	5/3	Mar	11	58.8	75.2	52.9	ERV	4.8	1205
416	11	7	7	11	7	11	9	15	12	2/3	Mar	6	59.4	68.4	58.6	ERV	4.3	1724
418 <sup>a</sup>	29	40	15	11	9	22	21	24	19	5/5	Mar/Apr	35	56.8	70.6	60.4	ERV	3.6	3107
420 <sup>a</sup>	33	18	22	29	26	20	25	24	16	5/4	Apr	41	54.8	66.5	58.3	Dehu	2.0	3017
421	11	0	24	9	18	11	12	15	12	2/3	Apr	24	55.6	60.9	63.0	CFIS	4.5	1334
422	18	15	9	2	9	9	10	15	12	2/3	Jul	27	60.2	70.5	74.8	CFIS	5.5	1206
424	20	9	22	24	22	13	18	15	12	2/3	Aug	44	58.6	84.9	76.6	None	5.9	1776
425	11	4	9	7	4	2	6	20	12	3/3	Aug	55	55.8	78.4	75.0	None	3.5	1828
427	7	9	11	11	9	13	10	15	12	2/3	Sep	14	44.4	49.8	57.0	None	4.0	1925
430	0	4	15	0	9	7	6	20	12	3/3	Oct	20	58.8	84.3	65.8	None	5.7	1800
431	37	11	9	24	0	0	14	24	16	5/4	Dec	6	56.2	75.4	50.0	None	3.2	2978
432 <sup>a</sup>	24	22	31	0	0	42	20	20	12	3/3	Dec	4	51.9	79.6	47.8	EXH	3.7	2200
435	35	29	9	7	15	9	17	20	12	3/3	Nov	5	60.8	75.3	56.8	None	3.9	1832
437	0	11	33	18	4	11	13	20	16	3/4	Dec	1	68.3	79.2	54.7	None	3.3	2536
440	22	31	22	9	7	9	17	20	19	3/5	May	38	52.0	60.9	63.0	None	3.9	3531
441	20	9	2	0	13	4	8	15	16	2/4	May	34	48.2	64.5	65.3	None	4.3	2580
442	0	15	15	2	0	0	6	15	12	2/3	Jun	63	58.3	72.5	70.5	Exh	4.1	1518
443	13	24	22	2	9	2	12	15	12	2/4	Jun	63	62.4	68.5	70.5	Exh	5.9	1600
444	15	15	4	20	26	13	16	15	12	2/3	Jul	26	60.2	71.2	67.3	None	4.7	1722
445 <sup>a</sup>	9	13	0	0	0	15	6	22	12	4/3	Jul	48	59.3	81.8	73.6	EXH	4.8	1650
446 <sup>a</sup>	0	9	0	9	13		6	15	12	1/3	Aug	29	52.3	87.9	76.6	None	5.0	1628
447 <sup>a</sup>	18	20	18	9	7	0	12	20	16	3/4	Sep	46	54.6	81.3	73.9	None	4.8	2285

<sup>a</sup>Default coefficients used for natural infiltration model rather than coefficients calibrated with tracer gas results.

As a result of the lab home validation showing the potential for larger error in the short-term daily IMG prediction, it is most useful to compare the six-day average generation rate to typical values used for design and simulation. Table 8 shows statistics for six-day average IMG rates for homes with differing occupancy. Figure 18 compares the six-day IMG averages and standard deviations to ASHRAE Standard 160-2021 values, which assume two occupants for the master bedroom, and one additional occupant for each additional bedroom. The ASHRAE Standard 160-2021 values are 70th percentile values, meaning 70% of homes with a corresponding number of occupants (or bedrooms) are expected to have an IMG rate lower than these values. Figure 18 shows that the ASHRAE Standard 160-2021 values generally fall at the upper end of the standard deviation, which is to be expected considering the standard deviation represents 68% of each sample. Referring back to Tables 6 and 7, seven of the 30 homes show six-day average IMG rates at or above the ASHRAE Standard 160-2021 rate. Only two homes exceed this rate by 20% or more (414 and 424).

Table 8. Six-day IMG statistics for homes of differing occupancy.

	<b>Number of Occupants</b>					
	<b>1</b>	<b>2</b>	<b>3</b>	<b>4</b>	<b>5</b>	<b>6</b>
Number of Homes	1	11	10	3	4	1
Six-day IMG Range kg/d (lb/d)	NA	3-8 (6-18)	3-10 (6-23)	3-13 (6-28)	6-11 (14-25)	NA
Six-day IMG Median kg/d (lb/d)	3 (6)	5 (10)	6 (14)	6 (14)	9 (19)	8 (6)
Six-day IMG Average kg/d (lb/d)	3 (6)	5.2 (11.5)	6.4 (14.1)	7.3 (16.0)	8.8 (19.3)	8 (17)
Six-day IMG Standard Deviation kg/d (lb/d)	NA	1.6 (3.6)	2.4 (5.2)	4.1 (9.1)	1.9 (4.1)	NA

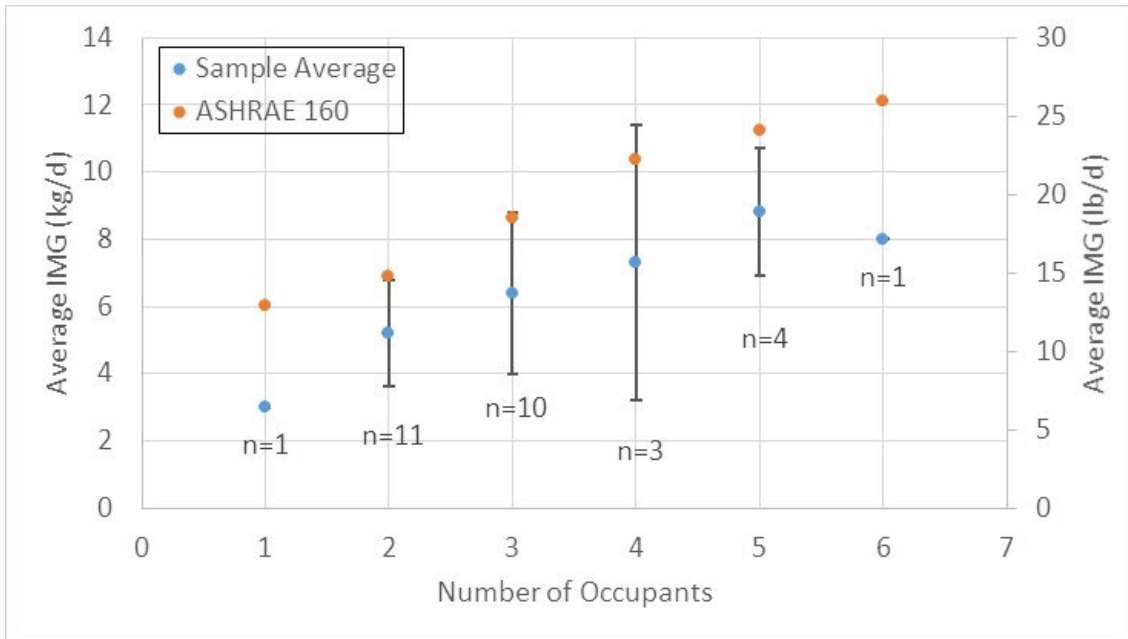


Figure 18. Average IMG rates per number of occupants.

Table 9 and Figure 19 show similar data based on number of bedrooms instead of number of occupants. In this figure, 6-day average IMG estimates are found to fall even further below the ASHRAE 160-2021 values. This is because, as seen in Table 10 and Figure 20, the occupied homes from this study, generally had less occupants per bedroom than what standards tend to assume.

Table 9. Six-day IMG rates for homes of differing numbers of bedrooms.

	Number of Bedrooms					
	1	2	3	4	5	6
Number of Homes	0	0	18	9	3	0
Six-day IMG Range kg/d (lb/d)	NA	NA	3-10 (6-23)	5-13 (11-28)	5-10 (11-22)	NA
Six-day IMG Median kg/d (lb/d)	NA	NA	5 (14)	6 (13)	8 (18)	NA
Six-day IMG Average kg/d (lb/d)	NA	NA	5.7 (12.5)	7.2 (15.8)	7.7 (16.9)	NA
Six-day IMG Standard Deviation kg/d (lb/d)	NA	NA	2.2 (4.8)	2.8 (6.2)	2.1 (4.6)	NA

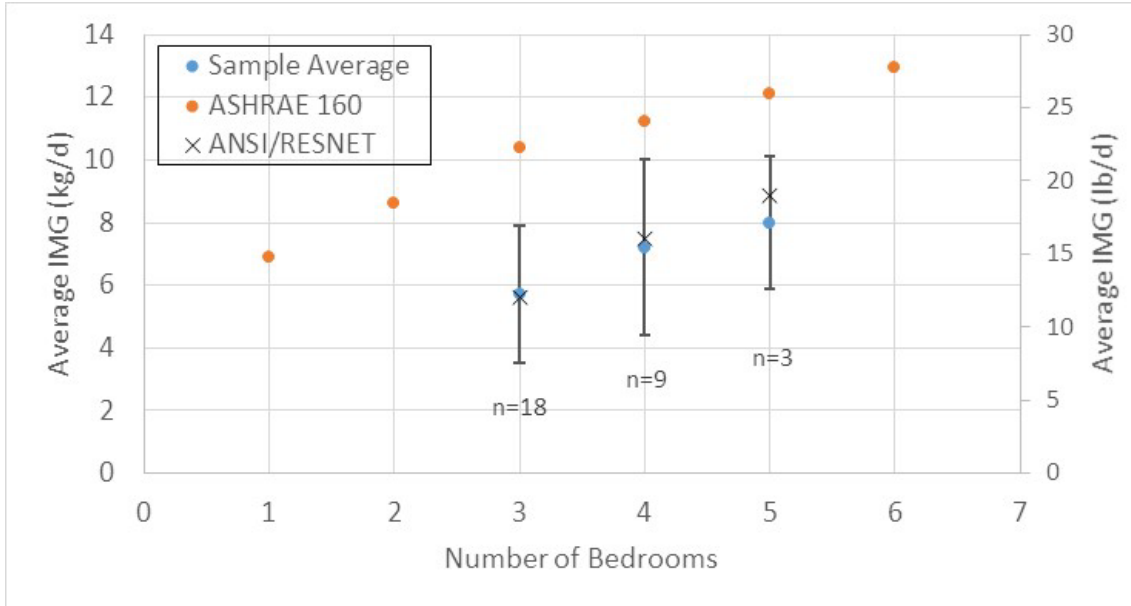


Figure 19. Average IMG rates per number of bedrooms.

Table 10. Occupancy statistics for homes with differing numbers of bedrooms.

	Number of Bedrooms					
	1	2	3	4	5	6
Number of Homes	0	0	18	9	3	0
Number of Occupants Range	NA	NA	1-5	2-6	2-5	NA
Number of Occupants Median	NA	NA	3	3	3	NA
Number of Occupants Average	NA	NA	2.7	3.7	3.3	NA
Number of Occupants Standard Deviation	NA	NA	0.9	1.3	1.2	NA

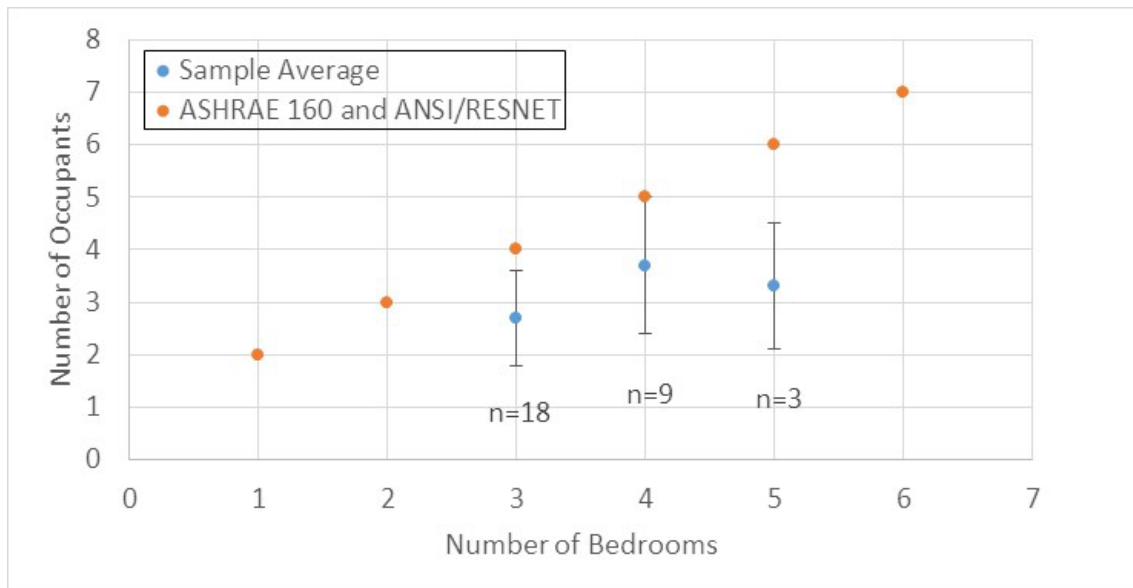


Figure 20. Number of occupants per bedroom.

Figure 19 also compares the 6-day average IMG estimates based on number of bedrooms to the ANSI/RESNET/ICC Standard 301 rates, used to represent a typical value for energy simulation purposes. Referring back to Tables 6 and 7, while 12 homes show six-day average IMG rates exceeding the ANSI/RESNET/ICC Standard 301 rates, with four homes exceeding this rate by 50% or more. The average values align very closely. However, one should consider that, as previously stated, the homes from this study generally had less occupants per bedroom than what standards tend to assume. Higher occupancy would likely result in 6-day average IMG estimates that exceed the ANSI/RESNET/ICC Standard 301 rates.

Except for five homes whose results show low weekly average IMG rates, all homes show 6-day average values within the range of values summarized by Glass and TenWolde (2009) and seen in Figure 1. While detailed error analysis is difficult to accomplish given the complexity of measured and calculated quantities, the laboratory validation estimates the error of the six day-average results to be 1.3-1.9 kg/d (2.9-4.2 lb/d).

## Conclusions

ASHRAE Research Project 1844 estimated IMG rates in 30 newer occupied homes built since 2013 in the southeastern US using a moisture balance model approach applied to six days of collected data in each home. Full-scale laboratory homes operating with known IMG rates were used to validate the moisture balance model and quantify the accuracy of estimates obtained when the model is applied to data from occupied homes with unknown IMG rates. In humid climates, air conditioning condensate, air exchange with outdoors, and diffusion can significantly contribute to an overall moisture balance, especially during summer months. During periods of varying indoor RH, moisture buffering of building materials and furnishings can also be a significant factor. It is difficult to make direct measurements of all moisture fluxes needed to accurately predict IMG rates with a moisture balance. For practicality, some moisture fluxes need to be estimated with indirect measurements, and both physics-based models and empirical models can be employed to estimate unknown parameters. Lab validation showed that the final moisture balance model could predict average IMG rates over a six-day period in the range of 1.3-1.9 kg/d (2.9-4.2 lb/d). Prediction error over the shorter term for individual days could be as high as 5 kg/d (11 lb/d).

IMG was found to vary from day to day in the occupied homes, as expected, likely resulting from occupancy and occupant behavior. As a result of the lab home validation showing the potential for larger error in the short term daily IMG prediction, it is most useful to compare the six day average generation rate to typical values used for design and simulation. With the exception of five homes whose results show low weekly average IMG rates, all homes show 6-day average values within the range of values summarized by Glass and TenWolde (2009) and seen in Figure 1.

Seven of the homes show six day average internal moisture generation rates at or above the ASHRAE Standard 160-2021 rate, which is a 70th percentile value, meaning 70% of homes with a corresponding number of occupants are expected have an internal generation rate lower than this value.. Only two homes exceed this rate by 20% or more. ASHRAE Standard 160-2021 values generally fall at the upper end of the standard deviations of the occupied home estimates, which is to be expected considering the standard deviation represents 68% of each sample. Twelve homes show six-day average internal moisture generation rates exceeding the ANSI/RESNET/ICC Standard 301 rate, used to represent a typical value for energy simulation purposes, with four homes exceeding this rate by 50% or more. However, the average values align very closely.

Results indicate that current design guidance for estimating IMG rates based on occupancy provided by ASHRAE Standard 160-2021, while initially based on occupied home datasets collected in the 1980s and 1990s, is still relevant when applied to newer homes. Results also show a trend that typical IMG values used by ANSI/RESNET/ICC Standard 301 for energy simulation purposes are also appropriate. However, it should be considered that the homes from this study generally had less occupants per bedroom than what standards assume. Higher occupancy would likely result in 6-day average IMG estimates that exceed the ANSI/RESNET/ICC Standard 301 rates.

## Nomenclature

$A$	= surface area of buffering, walls, ceiling, floor surfaces in the whole house, $m^2$
$\underline{g}$	= coefficients of linear model internal moisture generation correction term
$\bar{h}$	= vapor transfer coefficient, $m/s$
$A\bar{h}_{all}$	= product sum of surface area and vapor transfer coefficient, $m^3/s$
$\dot{m}_g$	= internal moisture generation rate of the whole house, $kg_{H_2O}/s$
$\dot{m}_{g,b}$	= internal moisture generation rate of the whole house with buffering term, $kg_{H_2O}/s$
$\Delta\dot{m}_{g,c}$	= internal moisture generation rate correction, $kg/s$
$\dot{m}_c$	= moisture removal rate by the air handling unit, $kg_{H_2O}/s$
$\dot{V}_V$	= ventilation plus infiltration air volume flow rate, $m^3/s$
$V_z$	= volume of air in the conditioned space house, $m^3$

$t$	= time, s
$\Delta t$	= time step, s
$P_{sat}$	= saturation pressure of water vapor at a given temperature, Pa
$P_{tot}$	= total pressure of the ambient, Pa
$R$	= gas constant of water vapor, 461.52 J/(kg·K)
$T$	= temperature of air or buffering material, K
$\Delta T_s$	= temperature difference used to estimate buffering material temperature, K
$\Delta x_s$	= thickness of the surface layer of the EMPD model, m
$\Delta x_d$	= thickness of the deep layer of the EMPD model, m
$\delta_v$	= water vapor permeability of buffering material, kg/(m·s·Pa)
$\rho_m$	= density of buffering material, kg/m <sup>3</sup>
$\rho_{air}$	= density of air, kg/m <sup>3</sup>
$\varphi$	= relative humidity, (-)
$\frac{du}{d\varphi}$	= slope of moisture sorption curve of buffering material, kg <sub>H2O</sub> /m <sup>3</sup>
$c$	= vapor density of moist air, kg <sub>H2O</sub> /m <sup>3</sup>
$c_z$	= vapor density of moist air in the conditioned space of the house, kg <sub>H2O</sub> /m <sup>3</sup>
$c_o$	= vapor density of outdoor air, kg <sub>H2O</sub> /m <sup>3</sup>
$c_s$	= vapor density of moist air at the buffering material surface, kg <sub>H2O</sub> /m <sup>3</sup>
$c_{attic}$	= vapor density of moist air in the attic space, kg <sub>H2O</sub> /m <sup>3</sup>
$c_{crawl}$	= vapor density of moist air in the crawl space, kg <sub>H2O</sub> /m <sup>3</sup>
$h_m$	= mass transfer coefficient, kg/m <sup>2</sup> s
$\dot{m}_{da,V}$	= total (ventilation plus infiltration) air mass flow rate, kg/s
$m_z$	= mass of the air in the whole house, kg
$\omega_z$	= humidity ratio of air node of the whole house, kg <sub>H2O</sub> /kg <sub>air</sub>
$\omega_o$	= humidity ratio of outdoor air, kg <sub>H2O</sub> /kg <sub>air</sub>
$\omega_s$	= humidity ratio of air at the surface of moisture absorbing material, kg <sub>H2O</sub> /kg <sub>air</sub>
$\omega_d$	= humidity ratio of air at deep layer of buffering material, kg <sub>H2O</sub> /kg <sub>DryAir</sub>
$t$	= time step

## Acknowledgements

This work was supported by the US Department of Energy, Office of Energy Efficiency and Renewable Energy, Buildings Technologies Office under Grant DE-EE0008186 and ASHRAE under Grant RP-1844.

## Disclosure Statement

The authors report there are no competing interests to declare.

## References

- ANSI 2019. ANSI/RESNET/ICC 301-2019, Standard for the Calculation and Labelling of the Energy Performance of Dwelling and Sleeping Units Using an Energy Rating Index
- ASHRAE 2021. ASHRAE 160-2021, Criteria for Moisture-Control Design Analysis in Buildings.
- ASHRAE 2022. ASHRAE 62.2-2022, Ventilation and Acceptable Indoor Air Quality in Residential Buildings.
- ASTM. 2017 ASTM E741-11, Standard Test Method for Determining Air Change in a Single Zone by Means of a Tracer Gas Dilution. Philadelphia: American Society for Testing and Materials.
- Boardman, C.R. and S. Glass. 2015. Basement Radon Entry and Stack Driven Moisture Infiltration Reduced by Active Soil Depressurization. *Building and Environment* 85 (2015) 220-232.
- Fang., X.; Christiansen, D.; Barker, G.; Hancock, E. 2011. Field Test Protocol: Standard Internal Load Generation for Unoccupied Test Homes. NREL/TP-550-51928. Golden, CO: National Renewable Energy Laboratory.
- Glass, S. and A. TenWolde. 2009. Review of Moisture Balance Models for Residential Indoor Humidity. 12th Canadian Conference on Building Science and Technology, Montreal, Quebec, 2009, pp. 231-246.
- Martin, E., T. Khan, J. Sonne, D. Chasar, C. Antonopoulos, S. Rosenberg, C. Metzger, W. Chen, B. Singer, M. Lubliner. Characterization of Mechanical Ventilation Systems in New US Homes: What types of systems are out there and are they functioning as intended? 2020 ACEEE Summer Study on Energy Efficiency in Buildings, Pacific Grove, CA, August 2020.
- Martin, E., B. Nigusse, C. Withers, Jr. and T. Khan. 2022. Lab Home Validation of a Moisture Balance Model to Estimate Internal Moisture Generation Rates in Occupied Homes. Conference Paper for 2021 ASHRAE Buildings XV Conference. Tampa, FL, December 2022.
- Pallin, S., Boudreaux, P., Jo, S. J., Perez, M., and Albaugh, A. 2017. Simulations of Indoor Moisture Generation in U.S. Homes. *Advances in Hygrothermal Performance of Building Envelopes: Materials, Systems and Simulations*,

ASTM STP159. ASTM International, West Conshohocken, PA, 2017, pp. 261–290.

Walker, I S, D J Dickerhoff, and M H Sherman. 2002. “The Delta Q Method of Testing the Air Leakage of Ducts.” 2002 ACEEE Summer Study on Energy Efficiency in Buildings, Pacific Grove, CA, August 2002.

Woods, J., J. Winkler, and D. Christensen. 2014. Using Whole House Field Tests to Empirically Derive Moisture Buffering Model Inputs. National Renewable Energy Laboratory NREL/TP-5500-62456. August, 2014.

Woods, J., and J. Winkler. 2018. Effective moisture penetration depth model for residential buildings: Sensitivity analysis and guidance on model inputs. *Energy & Buildings* 165 (2018) 216–232.

**Appendix A – Temperature Correction Values ( $\Delta T_s$  equation 4) and Internal Moisture Generation Correction Coefficients (for  $\Delta \dot{m}_{g,c}$  equation 5)**

Table A1 Vapor density at buffer material surface prediction detail linear model coefficients (SI).

<b>(To – Tz) range (C)</b>	<b>FRTF HOME</b>	<b>MHLAB</b>
$\geq 5$	5.85	5.00
$< 5, \geq 3$	5.41	4.84
$< 3, \geq 0$	4.97	5.15
$< 0, \geq -3$	5.37	6.38
$< -3, \geq -5$	6.22	6.39
$< -5$	8.29	5.84

Table A2 Coefficients of internal moisture generation correction linear equation model (SI).

<b>Coefficients</b>	<b>Units</b>	<b>FRTF HOME</b>	<b>MHLAB</b>
g0	kgH <sub>2</sub> O/s	-6.621	2.532
g1	kgDryAir/s	-103.600	-379.900
g2	kgDryAir/s	840.500	428.600
g3	kgH <sub>2</sub> O/ kgDryAir	-0.001	-0.005
g4	-	-0.120	-0.718
g5	-	0.143	0.502

## Appendix B – Analytical Solution to Estimate IMG with Diffusion and Application of Linear Model to Estimate Contribution of Moisture Buffering

The whole house moisture balance equation formulated using vapor density with and without moisture buffering term are given by:

$$V_z \frac{dc_z}{dt} = \dot{V}_V(c_o - c_z) + \dot{m}_g - \dot{m}_c + A\bar{h}_{buff}(c_s - c_z) + A\bar{h}_{ceil}(c_{attic} - c_z) + A\bar{h}_{wall}(c_o - c_z) + A\bar{h}_{crawl}(c_{crawl} - c_z)$$

$$V_z \frac{dc_z}{dt} = \dot{V}_V(c_o - c_z) + \dot{m}_g - \dot{m}_c + A\bar{h}_{ceil}(c_{attic} - c_z) + A\bar{h}_{wall}(c_o - c_z) + A\bar{h}_{crawl}(c_{crawl} - c_z)$$

These two equations are first order differential equations with constant coefficients and can be represented in a simplified form as follows:

$$c'_z = a \cdot c_z + b$$

If there is moisture buffer term the constant coefficients of the equation are given by:

$$a = -\left(\frac{\dot{V}_V}{V_z} + \frac{A\bar{h}_{ceil}}{V_z} + \frac{A\bar{h}_{wall}}{V_z} + \frac{A\bar{h}_{crawl}}{V_z} + \frac{A\bar{h}_{buff}}{V_z}\right)$$

$$b = \frac{\dot{V}_V}{V_z}c_o + \frac{\dot{m}_g}{V_z} - \frac{\dot{m}_c}{V_z} + \frac{A\bar{h}_{ceil}}{V_z}c_{attic} + \frac{A\bar{h}_{wall}}{V_z}c_o + \frac{A\bar{h}_{crawl}}{V_z}c_{crawl} + \frac{A\bar{h}_{buff}}{V_z}c_s$$

If there is no moisture buffering term, then the constant coefficients of the equation are given by:

$$a = -\left(\frac{\dot{V}_V}{V_z} + \frac{A\bar{h}_{ceil}}{V_z} + \frac{A\bar{h}_{wall}}{V_z} + \frac{A\bar{h}_{crawl}}{V_z}\right)$$

$$b = \frac{\dot{V}_V}{V_z}c_o + \frac{\dot{m}_g}{V_z} - \frac{\dot{m}_c}{V_z} + \frac{A\bar{h}_{ceil}}{V_z}c_{attic} + \frac{A\bar{h}_{wall}}{V_z}c_o + \frac{A\bar{h}_{crawl}}{V_z}c_{crawl}$$

The general analytical solution for this differential equation is as follows:

$$c_z^t = c_z^{t-1} \cdot e^{at} - \frac{b}{a} [1 - e^{at}]$$

Substituting for a and b coefficients and solving for internal moisture generation rate yields:

$$\begin{aligned} \dot{m}_g = \dot{m}_c - \dot{V}_V c_o - A\bar{h}_{ceil} c_{attic} - A\bar{h}_{wall} c_o - A\bar{h}_{crawl} c_{crawl} - A\bar{h}_{buff} c_s \\ + (\dot{V}_V + A\bar{h}_{ceil} + A\bar{h}_{wall} + A\bar{h}_{crawl} \\ + A\bar{h}_{buff}) \left[ \frac{c_z^t - c_z^{t-\Delta t} e^{\left(-\frac{\dot{V}_V + A\bar{h}_{ceil} + A\bar{h}_{wall} + A\bar{h}_{crawl} + A\bar{h}_{buff}}{V_z}\right)\Delta t}}{1 - e^{\left(-\frac{\dot{V}_V + A\bar{h}_{ceil} + A\bar{h}_{wall} + A\bar{h}_{crawl} + A\bar{h}_{buff}}{V_z}\right)\Delta t}} \right] \end{aligned}$$

The whole house internal moisture generation rate depends on knowledge of the whole house buffering material and exterior envelope diffusion surface areas, moisture transfer coefficients, vapor density at buffering material surface and the boundary conditions that includes outside air, crawl space, and the attic where applicable. In this investigation the attic air condition was replaced with outside air condition assuming the attic is fully vented.

Setting the moisture buffer term  $A\bar{h}_{buff}$  to zero the whole house base case (without the buffering term) internal moisture generation rate becomes:

$$\begin{aligned} \dot{m}_g = \dot{m}_c - \dot{V}_V c_o - A\bar{h}_{ceil} c_{attic} - A\bar{h}_{wall} c_o - A\bar{h}_{crawl} c_{crawl} \\ + (\dot{V}_V + A\bar{h}_{ceil} + A\bar{h}_{wall} \\ + A\bar{h}_{crawl}) \left[ \frac{c_z^t - c_z^{t-\Delta t} e^{\left(-\frac{\dot{V}_V + A\bar{h}_{ceil} + A\bar{h}_{wall} + A\bar{h}_{crawl}}{V_z}\right)\Delta t}}{1 - e^{\left(-\frac{\dot{V}_V + A\bar{h}_{ceil} + A\bar{h}_{wall} + A\bar{h}_{crawl}}{V_z}\right)\Delta t}} \right] \end{aligned}$$

One of the challenges of internal moisture generation prediction model has been estimation of buffering material moisture content. In a previous attempt an EMPD model to estimate moisture dynamics of buffering materials were investigated, which also required knowledge buffering material temperature history. In this alternative

approach, which includes diffusion through the envelope, moisture content of the buffering material was investigated by estimating the vapor density at buffering material surface using a linear model and is described next.

Rearranging the internal moisture generation prediction equation and solving for the vapor density at the buffering material surface yields:

$$c_s = \frac{1}{A\bar{h}_{buff}} (\dot{m}_c - \dot{m}_g - \dot{V}_V c_o - A\bar{h}_{ceil} c_{attic} - A\bar{h}_{wall} c_o - A\bar{h}_{crawl} c_{crawl}) + \left( \frac{(\dot{V}_V + A\bar{h}_{ceil} + A\bar{h}_{wall} + A\bar{h}_{crawl})}{A\bar{h}_{buff}} + 1 \right) \left[ \frac{c_z^t - c_z^{t-\Delta t} e^{\left( \frac{-\dot{V}_V + A\bar{h}_{ceil} + A\bar{h}_{wall} + A\bar{h}_{crawl} + A\bar{h}_{buff}}{V_z} \right) \Delta t}}{1 - e^{\left( \frac{-\dot{V}_V + A\bar{h}_{ceil} + A\bar{h}_{wall} + A\bar{h}_{crawl} + A\bar{h}_{buff}}{V_z} \right) \Delta t}} \right]$$

The vapor density at the buffering surface can be determined using the above formula from a long-term laboratory monitored data that includes boundary conditions (conditioned space air, outside air, attic space air, crawl space air), calculated infiltration air flow rate per ASHRAE 62.2, measured ventilation air flow rate, measured internal moisture generation rate, measured condensation and assumed vapor transport coefficients for the walls, ceilings, and floors assemblies of the FSEC laboratory homes. The estimated vapor density was fit to linear model as a functions of characteristics of the two FSEC's laboratory homes. A detailed and simple linear model equation for predicting vapor density at the buffering material surface were formulated and investigated.

Detailed linear model for predicting vapor density at the buffering material surface consists of known parameters and measured variables including actual internal moisture generation rate is given by:

$$c_s = a_0 + a_1 \frac{\dot{m}_c}{A\bar{h}_{all}} + a_2 \frac{\dot{V}_V c_o}{A\bar{h}_{all}} + a_3 \frac{\dot{V}_V c_z}{A\bar{h}_{all}} + a_4 V_z c_z + a_5 \frac{\dot{m}_g}{A\bar{h}_{all}} + a_6 c_o$$

The constant coefficients of the detailed linear model equation are provided in Table B1. A simple linear model for predicting buffering material surface vapor density consist of whole house ventilation and infiltration air flow rate, and indoor and outside air vapor densities as input variables is given by:

$$c_s = a_0 + a_1 \dot{V}_V c_o + a_2 c_z + a_3 c_o$$

The coefficients of the simple linear model equation are provided in Table B2. The simple model was intended for field home application where detailed measured data may not be available.

Table B1 Vapor density at buffer material surface prediction detail linear model coefficients (SI).

Detailed Linear Model	Units	FRTF Home		MHLAB	
		With Internal Moisture Gen	Without Internal Moisture Gen	With Internal Moisture Gen	Without Internal Moisture Gen
a0	kgH2O/m <sup>3</sup>	0.0012541	0.0133000	-0.0004570	0.0008103
a1	-	0.8638709	0.2557000	0.1448940	0.0870745
a2	-	-0.8821085	-0.2145000	0.0605140	0.1454902
a3	-	0.8935465	0.2152000	0.0395020	-0.0283256
a4	1/m <sup>3</sup>	0.0021731	0.0000071	0.0021730	0.0015888
a5	-	-0.8762935	0.0	-0.5206370	0.0
a6	-	0.0000000	-0.3655000	0.0143060	0.0164024

Table B2 Vapor density at buffer material surface prediction simple linear model coefficients (SI).

<b>Simple Linear Model</b>	<b>Units</b>	<b>FRTF Home</b>	<b>MHLAB</b>
a0	kgH2O/m <sup>3</sup>	0.00966900	-0.00088580
a1	s/m <sup>3</sup>	-0.00000031	0.00000092
a2	-	0.35640000	0.60410000
a3	-	-0.22190000	0.30030000

Nomenclature:

$A$	=	surface area of buffering, walls, ceiling, floor surfaces in the whole house, m <sup>2</sup>
$\bar{h}$	=	vapor transfer coefficient, m/s
$A\bar{h}_{all}$	=	product sum of surface area and vapor transfer coefficient, m <sup>3</sup> /s
$\dot{m}_g$	=	internal moisture generation rate of the whole house, kgH2O /s
$\dot{m}_c$	=	moisture removal rate by the air handling unit, kgH2O /s
$\dot{V}_V$	=	ventilation plus infiltration air volume flow rate, m <sup>3</sup> /s
$V_z$	=	volume of air in the conditioned space house, m <sup>3</sup>
$t$	=	time, s
$\Delta t$	=	time step, s
$c$	=	vapor density of moist air, kgH2O/m <sup>3</sup>
$c_z$	=	vapor density of mist air in the conditioned space of the house, kgH2O/m <sup>3</sup>
$c_o$	=	vapor density of outdoor air, kgH2O/m <sup>3</sup>
$c_s$	=	vapor density of moist air at the buffering material surface, kgH2O/m <sup>3</sup>
$c_{attic}$	=	vapor density of moist air in the attic space, kgH2O/m <sup>3</sup>
$c_{crawl}$	=	vapor density of moist air in the crawl space, kg

## Appendix C – Additional Home Specific Data

Table C1 Additional home specific data (SI).

Home #	Data Collection Month	Average Daily Condensate (kg/d)	Average Indoor RH (%)	Average Outdoor RH (%)	WHV Type	ACH50	Floor Area (m <sup>2</sup> )
402	Oct	24	49.9	79.0	None	2.9	248
403	Oct	20	54.9	78.2	None	4.1	196
405	Nov	8	62.6	76.7	ERV	3.7	191
408	Dec	0	54.2	87.6	None	1.7	293
409	Jan	0	55.6	75.4	None	5.4	183
410	Jan/Feb	0	54.4	69.9	None	1.8	360
411	Feb	9	60.8	71.4	None	4.0	149
414	Feb/Mar	21	53.7	83.5	Dehu	2.3	270
415	Mar	5	58.8	75.2	ERV	4.8	112
416	Mar	6	59.4	68.4	ERV	4.3	1724
418	Mar/Apr	16	56.8	57.8	ERV	3.6	289
420	Apr	19	54.8	65.7	Dehu	2.0	281
421	Apr	11	55.6	60.9	CFIS	4.5	124
422	Jul	12	60.2	70.5	CFIS	5.5	112
424	Aug	20	58.6	84.9	None	5.9	165
425	Aug	25	55.8	81.3	None	3.5	170
427	Sep	6	44.4	49.8	None	4.0	179
430	Oct	9	58.8	84.3	None	5.7	167
431	Dec	3	56.2	75.4	None	3.2	277
432	Dec	2	51.9	79.6	EXH	3.7	205
435	Nov	2	60.8	75.3	None	3.9	170
437	Dec	0	68.3	79.2	None	3.3	236
440	May	17	52.0	62.9	None	3.9	328
441	May	15	48.2	64.5	None	4.3	240
442	Jun	29	58.3	72.5	Exh	4.1	141
443	Jun	29	62.4	68.5	Exh	5.9	149
444	Jul	12	60.2	71.2	None	4.7	160
445	Jul	22	59.3	81.8	EXH	4.8	153
446	Aug	13	52.3	87.9	None	5.0	151
447	Sep	21	54.6	81.3	None	4.8	213

Table C2 Additional home specific data (IP).

Home #	Data Collection Month	Average Daily Condensate (lb/d)	Average Indoor RH (%)	Average Outdoor RH (%)	WHV Type	ACH50	Floor Area (ft <sup>2</sup> )
402	Oct	53	49.9	79.0	None	2.9	2670
403	Oct	44	54.9	78.2	None	4.1	2104
405	Nov	18	62.6	76.7	ERV	3.7	2055
408	Dec	0	54.2	87.6	None	1.7	3150
409	Jan	0	55.6	75.4	None	5.4	1967
410	Jan/Feb	0	54.4	69.9	None	1.8	3869
411	Feb	20	60.8	71.4	None	4.0	1597
414	Feb/Mar	46	53.7	83.5	Dehu	2.3	2900
415	Mar	11	58.8	75.2	ERV	4.8	1205
416	Mar	6	59.4	68.4	ERV	4.3	1724
418	Mar/Apr	35	56.8	57.8	ERV	3.6	3107
420	Apr	41	54.8	65.7	Dehu	2.0	3017
421	Apr	24	55.6	60.9	CFIS	4.5	1334
422	Jul	27	60.2	70.5	CFIS	5.5	1206
424	Aug	44	58.6	84.9	None	5.9	1776
425	Aug	55	55.8	81.3	None	3.5	1828
427	Sep	14	44.4	49.8	None	4.0	1925
430	Oct	20	58.8	84.3	None	5.7	1800
431	Dec	6	56.2	75.4	None	3.2	2978
432	Dec	4	51.9	79.6	EXH	3.7	2200
435	Nov	5	60.8	75.3	None	3.9	1832
437	Dec	1	68.3	79.2	None	3.3	2536
440	May	38	52.0	62.9	None	3.9	3531
441	May	34	48.2	64.5	None	4.3	2580
442	Jun	63	58.3	72.5	Exh	4.1	1518
443	Jun	63	62.4	68.5	Exh	5.9	1600
444	Jul	26	60.2	71.2	None	4.7	1722
445	Jul	48	59.3	81.8	EXH	4.8	1650
446	Aug	29	52.3	87.9	None	5.0	1628
447	Sep	46	54.6	81.3	None	4.8	2285